8-1961

A Study of Catalytic Reactions on Semiconductors: Hydrogen Deuterium Exchange and Formic Acid Decomposition on Chemically-Doped Germanium

George Edward Moore
University of Tennessee - Knoxville

To the Graduate Council:

I am submitting herewith a dissertation written by George Edward Moore entitled "A Study of Catalytic Reactions on Semiconductors: Hydrogen Deuterium Exchange and Formic Acid Decomposition on Chemically-Doped Germanium." I have examined the final electronic copy of this dissertation for form and content and recommend that it be accepted in partial fulfillment of the requirements for the degree of Doctor of Philosophy, with a major in Chemistry.

Hilton A. Smith, Major Professor

We have read this dissertation and recommend its acceptance:

Ellison H. Taylor, James Crawford, William J. Smith, C. W. Kennan

Accepted for the Council:

Carolyn R. Hodges

Vice Provost and Dean of the Graduate School

(Original signatures are on file with official student records.)

August 8, 1961

To the Graduate Council:

I am submitting herewith a thesis written by George Edward Moore entitled "A Study of Catalytic Reactions on Semiconductors: Hydrogen-Deuterium Exchange and Formic Acid Decomposition on Chemically-Doped Germanium:" I recommend that it be accepted in partial fulfillment of the requirements for the degree of Doctor of Philosophy, with a major in Chemistry.

Hilton A. Smith
Major Professor

We have read this thesis and
recommend its acceptance:

Ellison H. Taylor
James L. Crawford Jr.
Wm. J. Smith Jr.
C. W. Kiernan

Accepted for the Council:

L. R. Spivey
Dean of the Graduate School

A STUDY OF CATALYTIC REACTIONS ON SEMICONDUCTORS: HYDROGEN-DEUTERIUM EXCHANGE AND FORMIC ACID DECOMPOSITION ON CHEMICALLY-DOPED GERMANIUM

A Dissertation

Presented to

the Graduate Council of

The University of Tennessee

In Partial Fulfillment

of the Requirements for the Degree

Doctor of Philosophy

---

by

George Edward Moore

August 1961

To N. W. M.

ACKNOWLEDGMENT

The author wishes to express his sincere gratitude to Professor Hilton A. Smith and Dr. Ellison H. Taylor for their counsel and encouragement during the course of this research. Thanks are also due Dr. James H. Crawford, Jr. for helpful discussions, Dr. C. O. Thomas, Dr. J. W. Nielsen and Mr. John W. Cleland for samples of germanium, Mr. W. D. Harman and Mrs. Mary G. Davis for mass spectrometry, Dr. H. W. Kohn for helpful cooperation, Mr. Paul Dake for surface area measurements, and Mrs. Virginia Lee for secretarial services.

This research was carried out at the Oak Ridge National Laboratory operated for the United States Atomic Energy Commission by Union Carbide Nuclear Company.

TABLE OF CONTENTS

LIST OF TABLES

LIST OF FIGURES

FIGURE PAGE

CHAPTER I

INTRODUCTION

A. General

Berzelius in 1836 wrote about "some ideas on a new force which acts in organic compounds."[1] He called this force *force catalytique* and gave the name *catalyse* to the phenomenon of "decomposition of bodies by this force."

Since Berzelius, progress in the science of catalysis has been observed to conform to the development of an autocatalytic reaction;[2] the contributions of Faraday and Sabatier produced the early, gently accelerating progress, but at the start of the present century the curve of progress took a sharp, upward autoaccelerative turn. Both I. Langmuir's basic contributions and the success of technical catalytic processes were believed responsible by H. S. Taylor[2] for the phenomenal growth of this field in the last 45 years.

The *force catalytique* was at first regarded as a mysterious phenomenon, since a relatively small amount of catalyst could influence greatly the rate of reaction of a very large amount of material without itself undergoing change. Many investigators sought to identify the forces in the catalyst responsible for such activity.

Berzelius wrote that he did not believe that the *force catalytique* was "entirely independent of the electrochemical affinities of matter."[1] Langmuir, at a meeting of the Faraday Society in 1921, spoke especially

of the geometrical arrangement of atoms in the surface of an active catalyst, but noted that "if these atoms are a little too far apart, or if their electrons are not sufficiently mobile to permit of the electron rearrangement involved in surface reactions, the reaction will be retarded."[3] H. S. Taylor introduced the concepts of "active centers"[4] and "activated adsorption";[5] the latter brought out the electronic factor while the concept of active centers considered chemical adsorption and initiation of reaction through energetic and geometric processes. Thus, in the earliest stages of the development of heterogeneous catalysis, both electronic and geometric factors of the solid were recognized as possible sources of catalytic activity.

Determination of precise relationships between the electronic factor or the geometric factor in controlling catalytic activity has been attempted by many investigators. Balandin[6] and Beeck[7] were early contributors to studies of the geometrical factor while more recently experiments on chemisorption and catalysis on various faces of single crystals by Gwathmey[8] and Sosnovsky[9] have added to this knowledge. The geometric factor is concerned primarily with the surface structure of the catalyst and suggests that a particularly favorable fit of adsorbed molecules on the array of atoms in the crystal surface will promote reaction. Differences in catalytic activity between different faces of one catalyst with specific electronic character were found to be much greater than activity differences between catalysts of appreciably different electronic character.[8]

On the other hand, electronic interactions between the solid and the reacting molecules were suggested as being responsible for chemisorption

and catalytic reaction, and these ideas of catalysis became expressed as the "electronic factor"[10] which will be discussed in the next section.

However, a clear-cut separation of geometric and electronic factors was not evident in many cases. For example, rates for the hydrogenation of ethylene on evaporated films of the transition metals[11] could be correlated either with the lattice spacing[11] or the per cent d-character of the metallic bond.[12] The reason for this now appears to be the dependence of lattice spacing on d-character.[13]

There seems no a priori reason why these two factors must be mutually exclusive. Electronic properties vary with crystal face, as illustrated in the variation of the work function, which is a measure of the electron affinity of a metal, with crystal face.[14] It seems reasonable, therefore, to expect that electronic interactions between the solid and the reacting molecules might be related in some fashion to the crystal face of the solid, since the electronic properties at the surface of the solid depend in part on the arrangement of atoms with respect to each other in the surface layer.[15]

One way to investigate the relationships between the geometric and electronic factors and catalytic activity is to study the effect of each factor separately; ideally, one factor is kept constant, while the other is varied. The dependence of a catalytic reaction on crystal face may be determined using a single crystal as the catalyst. If the crystal is sufficiently large, rates of reaction on the different faces may be measured.[8]

Dependence of catalytic activity on electronic factors may be studied with a series of samples possessing varying electronic properties, but with chemical and other physical properties constant. However, this situation has been difficult to realize experimentally. The availability of elemental semiconductors of unprecedented quality has provided an attractive method of being able to study, better than heretofore possible, the relationship between electronic factors and catalytic activity, independent of geometric factors. To understand this situation better, the electronic factor in catalysis will be considered in a little more detail.

B. The Electronic Factor

Chemisorption, per se, and as a precursor to heterogeneous catalytic reaction, focused attention on the bond between surface and adsorbate and led to considerations of the electronic factor. The transfer of electrons to effect ionization of adsorbed species was considered by Brewer,[16] Schmidt,[17] Nyrop[18] and others[19] in the period 1928 to 1937. In 1928, Roginskii and Shul'tz[20] considered the role of electrons in catalytic decomposition, and, in 1932, Lennard-Jones[21] considered the possibility of covalent bond formation by electron pairing between the adsorbed atom and a metal. In 1940, Emmett and Teller[22] cautioned against a wholesale acceptance of ions on the surface as the explanation of all contact catalysis, and suggested in turn that electron sharing or transitional electronic interactions may be operative.

In 1938, Wagner and Hauffe[23] demonstrated an actual transfer of electrons between a reactant and a solid in a heterogeneous catalytic reaction. In 1944, Schwab published the first[24] in a series of papers[25] showing a definite relationship between electron density in a series of alloys and the activation energy of the surface-catalyzed decomposition. Schwab postulated a donor-acceptor relation with respect to electrons between the solid and the chemical species adsorbed on the surface.

Dowden[26] in 1950 proposed to consider heterogeneous catalysts as metals, semiconductors, or insulators in seeking the interrelationships between electronic structure of the solid and catalysis. This illuminating discussion helped clarify the role of the electronic factor in chemisorption and catalysis. Trapnell[27] reviewed this position for metallic catalysts while Stone,[28] Hauffe,[29] Wolkenstein[30] and others[31, 32] have contributed greatly to the knowledge of the electronic factor in chemisorption and catalysis on semiconductors.

Electronic interactions between adsorbate and adsorbent during chemisorption can perhaps be seen better by consideration of the following examples.[33] If the foreign molecule to be adsorbed on a surface of a solid possesses a completed shell of electrons and has no electron affinity and is only slightly polarizable (e.g., a rare gas atom), electron transfer upon adsorption is not apt to occur, but there can be a small electronic shift if the solid has sufficiently great electron affinity. On the other hand, if the electron affinity (work function) of the solid is low with respect to that of the foreign molecule, an electron shift from the solid to the adsorbate (e.g., oxygen atom) may occur; the reverse condition of the

electron affinity of the solid being high with respect to that of the foreign molecule may result in an electron transfer from the adsorbate (e.g., hydrogen atoms) to the solid. There are many intermediate cases between these limiting examples, of course, and the extent and manner of the electronic interaction can be variously described as electrons shifts, partial or complete transfers, ionizations, covalent bondings, or polarizations. In addition, electrons can be transferred from a foreign species to a solid (e.g., from hydrogen atoms to a metal such as platinum with high electronic work function) or from a different solid to the same foreign species (e.g., from alkali-metal surfaces to hydrogen atoms). Imposed upon these complexities of electronic interactions may be secondary influences of a geometric or steric or defect nature.

During those years when the electronic factor in chemisorption and catalysis was being developed, a clearer understanding of solids was being brought about through developments in quantum mechanics and their application to solids. Progress in understanding semiconducting properties of solids originated in the theory of electronic semiconductors proposed by A. H. Wilson[34] in 1931; the availability of high-purity, single crystals of germanium and silicon has permitted a thorough investigation of these ideas. As a result, a clearer understanding of chemical processes during heterogeneous catalysis on semiconducting solids has been possible.

The introductory remarks by P. B. Weisz[35] at the Conference on the Physics of Semiconductor Surfaces in Philadelphia in 1956 were entitled "Bridges of Physics and Chemistry Across the Semiconductor Surface." It was pointed out that the boundary of a solid is not so much the dividing

line between physics and chemistry as it is a meeting ground of mutual interest and importance. The surface is the bridge between the physicist's attention to the behavior of the electrical carriers (electrons and holes) within the solid and the chemist's concern with its influence on the atmosphere of atoms and molecules externally surrounding the solid.

Since this is precisely the broad area of concern in this thesis, one might well inquire into past developments in this field.

The main knowledge of chemisorption and catalysis on semiconductors has stemmed from studies with metallic oxides. This work can be described only as monumental. Yet, the utility of metallic oxides as catalysts in fundamental studies is limited. Perhaps the most serious disadvantage is that each oxide is a single-carrier semiconductor, i.e., its semiconductivity is normally always n-type (excess electron) or p-type (excess hole). Chemical doping of the crystal can change the concentration but not the type of majority charge carrier. To employ different types of semiconductivity requires that chemically different metallic oxides be used.

Semiconducting oxides that depend on nonstoichiometry for their electronic properties suffer from the disadvantage that their deviations from stoichiometry and, therefore, their electronic properties, are sensitive to the atmosphere. Although incorporation of impurity foreign atoms can be used to control the electronically active centers, concentrations up to 5 mole per cent foreign atom are frequently required so that changes in properties of the catalyst, other than just electronic, become likely.[36]

On the other hand, elemental semiconductors (e.g., germanium) appear eminently suited to probe the relationship between chemisorption or contact catalysis and electronic properties of the solid. Purely electronic effects may be dealt with without complications from ionic factors. These semiconducting metalloids are chemically homogeneous solids possessing double-carrier semiconductivity, i.e., n- and p-type extrinsic semiconductivity can be achieved by incorporating certain foreign atoms into the host lattice. Only extremely small concentrations of impurities, when homogeneously dispersed, are necessary to alter the concentration of charge carriers by orders of magnitude, while producing almost undetectable changes in bulk chemical and physical properties. By such means, the semiconductivity of the solid can be varied from p- to n-type without concomitant changes in other variables. Thus, elemental semiconductors appear better suited than oxides as adsorbents or catalysts to ascertain the influence of this single parameter.

Although the value of investigations using elemental semiconductors in chemisorption and catalysis has been recognized,[37, 38] the techniques of chemistry and metallurgy have only recently succeeded in producing elemental germanium, and other elemental semiconductors, as pure, single crystals. Purified germanium containing controlled amounts of appropriate impurity atoms has been available only within the last five years, and, therefore, its use in catalytic studies has been very limited.

The purpose of the research which is described in this thesis was to explore intensively and, thereby, to clarify the relationship between heterogeneous catalytic activity and the semiconductivity of the solid through the use of a two-carrier, elemental, semiconducting catalyst. This was

accomplished by determining the dependence of kinetic factors for two typical heterogeneous reactions-the exchange of hydrogen with deuterium and the catalytic decomposition of formic acid vapor-on the electronic chemical potential of chemically-doped germanium.

C. Previous Catalytic Studies with Germanium

Germanium metal and its compounds have been used very little as catalysts. This is quite understandable for these materials appear not to possess unusual catalytic properties. Metallic germanium has been studied as a catalyst from two points of view: one concerns its intrinsic catalytic activity and the other is connected with its properties as a semiconductor.

Metallic germanium, per se, was apparently first studied as a catalyst in 1932 by Hogness and Johnson[39] who catalytically decomposed germane on a germanium surface. The thermal decomposition of germane,[40, 41] arsine,[40] and ammonia[42] on germanium films has been investigated more recently by a group at Princeton University.[43]

The hydrogen-deuterium exchange on germanium films also has been studied by the Princeton group,[41, 43, 44] and although no catalytic activity was observed at first, improved experimental techniques did demonstrate the ability of such surfaces to catalyze the exchange.[45] The exchange has been determined in this same temperature range (300° to 550°) on crushed single crystals,[46] and at low temperature (77°K.) on sputtered films.[47] The parahydrogen conversion at low temperatures was also studied.[47]

Germanium filaments upon flashing were found to decompose methyl alcohol into carbon monoxide and hydrogen.[48] Methyl and isopropyl alcohols have been catalytically dehydrated on crushed germanium in the temperature range 100° to 150°.[49] The decomposition of nitrous oxide at 180° into nitrogen and oxygen upon freshly evaporated germanium,[50] the catalytic oxidation of carbon monoxide,[51] and the decomposition of formic acid vapors[51] have all been related to changes in the work function of germanium.

Many of these investigations showed that metallic germanium was the active catalyst and that exposure to air or oxygen destroyed or greatly reduced the activity. Thus, hydrogen-deuterium exchange was found to occur at low temperatures only on atomically clean surfaces and was observed to be almost completely quenched on oxygen-contaminated films.[47] Oxygen, which was produced in the decomposition of nitrous oxide, was found to poison the germanium surface for this reaction.[50] Oxidations of hydrogen to water or of carbon monoxide to carbon dioxide with oxygen were not observed at 200° to 400° because of selective adsorption of oxygen on the metal.[49] Germanium powder, presaturated with oxygen at 25°, was also unable to promote these oxidations.[52]

Industrially, metallic germanium has been considered for a hydrogenation catalyst for carbonaceous materials,[53] as a catalyst in the production of highly polymeric polymethylene terephthalates,[54] and in the catalytic preparation of an alumina hydrosol.[55]

Chemically-doped, semiconducting germanium has not been available until very recently and its use in catalytic studies has been limited to one publication each from Germany, Russia and the United States.

G. M. Schwab, who has been a foremost investigator of catalysis and semiconductivity, and his co-workers were first to utilize the semiconducting properties of chemically-doped elemental germanium for studies in heterogeneous catalysis.[37, 56] Penzkofer studied the dehydrogenation of formic acid vapor on n- and p-type germanium and found that on freshly etched surfaces the activation energy was smaller (33 kcal./mole) for p-type than for n-type (42 kcal./mole) and was intermediate (37 kcal./mole) for intrinsic germanium. Krawczynski studied the hydrogenation of ethylene and found that the reaction on p-type germanium started near 100° and proceeded with an activation energy of 3 kcal./mole, whereas on n-type germanium the reaction became measurable only near 375° with an activation energy near 22 kcal./mole. In both studies, no significant change in activation energy was observed for 300-fold changes in carrier concentration (impurity concentration range, 10^{18} to 10^{20} atoms/cm.^{3}). Silicon and Group III-V intermetallic compounds were also studied and, in general, gave similar results.

Chemically-doped germanium has also been used for the catalytic dehydrogenation of ethanol.[57] The activation energy on undoped germanium was 23.5 kcal./mole, increased to 27.5 kcal./mole on antimony-doped germanium (n-type), and decreased to 18 kcal./mole on gallium-doped germanium (p-type). There was no significant change in activation energy within a 500-fold change in antimony concentration or within a 2000-fold change in gallium doping. Samples with the lowest concentrations of doping ($\sim 10^{15}$ atoms/cm.^{3}) would be expected to have behaved as intrinsic semiconductors in the temperature range used (200° to 270°).

The catalytic activity of p- and n-type germanium in the Friedel-Crafts reaction has recently been determined.[58] P-type germanium was much more active than n-type. Activation energies were not reported.

In these studies with chemically-doped germanium, greatly decreased catalytic activity after exposure to oxygen or air was also reported.

Adsorption of gases on germanium has been extensively studied. Rare gases were not adsorbed at room temperature, and carbon monoxide, carbon dioxide, and nitrogen were only physically adsorbed.[48, 52, 59] Oxygen was readily chemisorbed at room temperature;[52, 60, 61] the rate and extent of adsorption appeared to be independent of the type of semiconductivity.[52, 62] Molecular hydrogen apparently was not adsorbed on germanium[45, 52, 61] whereas atomic hydrogen was adsorbed.[48, 61] Adsorption of organic vapors[61] and some preliminary studies on the adsorption of propanol and acetic acid on n- and p-type germanium[63] have been reported.

D. Solid State Principles

Application of solid state principles to catalytic solids has been gratifyingly successful in revealing relationships between electronic properties of solids and heterogeneous catalysis. However, the solids used as catalysts have not always been so well understood, nor have the systems been so simple, that unambiguous results always were obtained. In the research to be described in the next chapter, one of the better understood and controlled semiconducting solids was employed as the catalyst. It was hoped that by using a solid whose electronic properties were

well understood, and by determining the behavior of well-known catalytic reactions on its surface, a meaningful contribution to the knowledge of heterogeneous catalysis would result.

It is appropriate to review briefly from a chemical point of view some of the modern concepts of the solid state, emphasizing semiconductors, especially germanium. No attempt will be made to develop the quantum mechanical details of the motion of electrons (and holes) in crystals. An American Chemical Society monograph[64] has recently been published about semiconductors and describes the subject very well indeed.

Electronic interactions between solids and adsorbates are conveniently discussed in terms of the band theory, and a brief description of this theory serves as a point of departure for this section.

1. Band Theory of Solids

Consider an assembly of atoms arranged in space in a geometric pattern equivalent to some crystal lattice, but with interatomic distances so large that there is no interaction between the atoms. Each atom may be regarded as isolated and the electron energy levels remain discrete or quantized. If the atoms are brought closer together, these electron energy levels become modified, for when the interatomic distance becomes sufficiently small, the wave functions of outer electrons of each atom begin to interact with one another. This results in a splitting of the energy levels, i.e., levels differing in energy by a small amount are formed.

When this idea is extended to the large assembly of atoms forming a crystalline array, the discrete energy levels corresponding to the

quantum states of the isolated atoms split into groups of levels so closely spaced that they form an almost continuous energy band. This is illustrated in Figure 1. The bands formed from the various levels may be separated or they may overlap. There are no quantum states with energies between those in the bands, and the energy range between such allowed energy bands is known as the forbidden energy band or gap.

The inner electrons of atoms can be considered to be unaffected in the crystal since no appreciable overlapping of their wave functions occurs. The outermost valence electrons are affected as just described and lead to a representation of band structure of solids as illustrated in Figure 2.

Electrons in solids can contribute to an electric current only if they can move in a partially empty band. If all the available energy states of a band are occupied by electrons (a "full" band), the electrons cannot function as current carriers. Free charge carriers may be produced by thermally or optically exciting electrons into the next higher band which may be empty or almost so. If the gap between the bands (the forbidden energy gap) is wide, the activation would be possible only at high temperatures and the solid would be regarded as an insulator at room temperature. The empty or only partially-filled band is called the "conduction" band and the electrons in it are regarded as being almost (quasi-) free charge carriers. If the forbidden gap is relatively small (<1 e.v.), transfer of electrons from the filled band to the conduction band can occur at moderate temperatures and the solid is known as an intrinsic semiconductor (Figure 2). Transfer of an electron from the filled

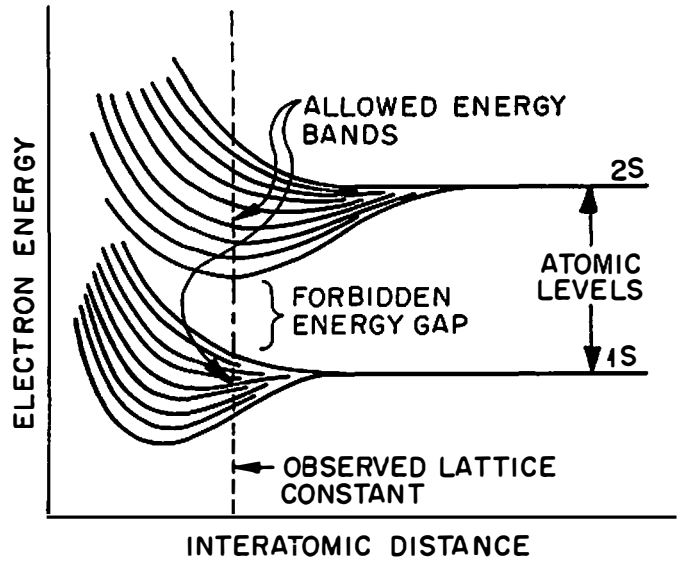

Figure 1. Formation of energy bands. (Schematic)

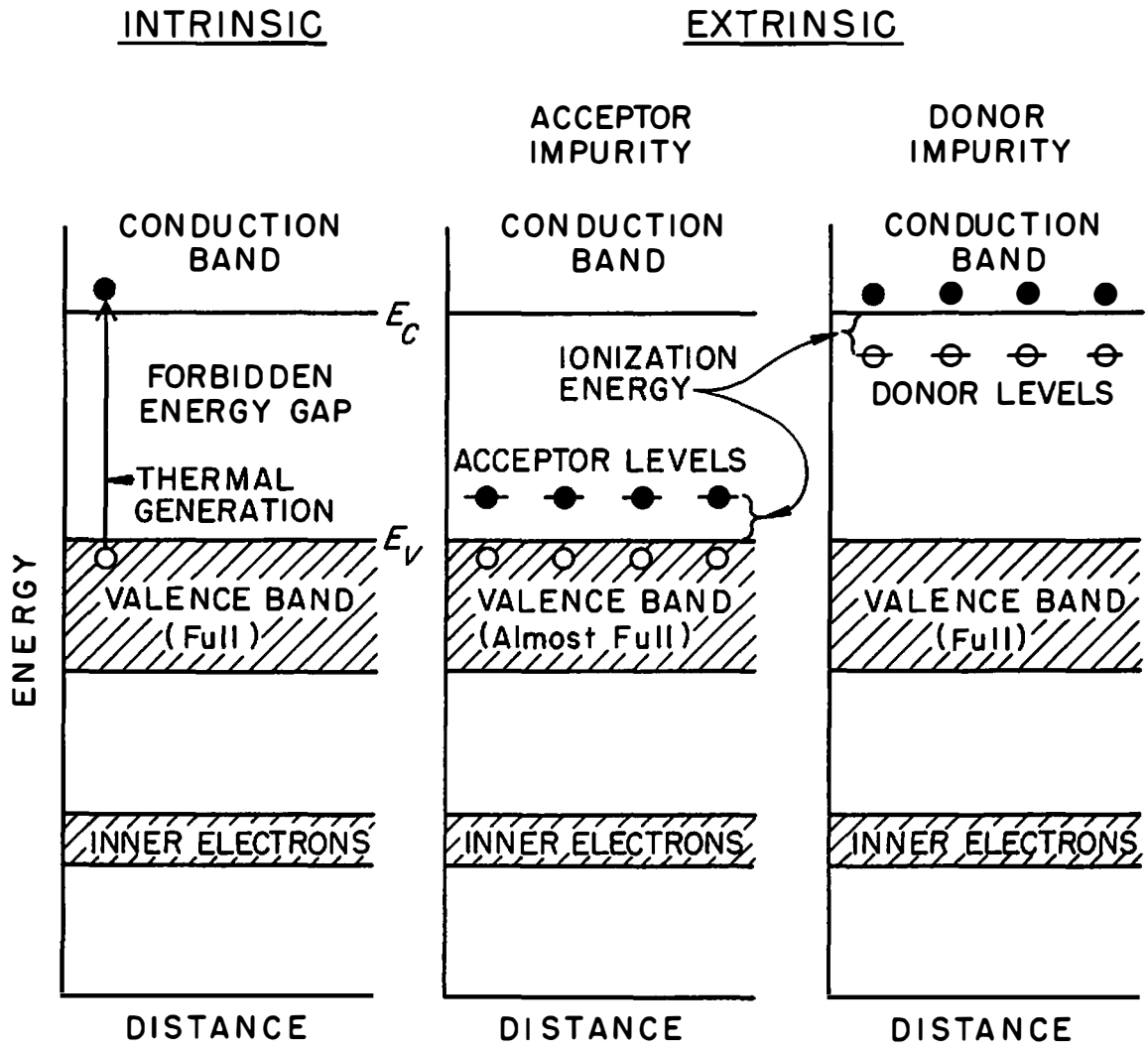

Figure 2. Band structure of semiconductors.

(valence) band leaves an electron deficiency or vacancy which is referred to as a "positive hole." Since the valence band is not now completely full of electrons, electrons can move into the vacancy; it becomes convenient, however, to regard the hole as being in motion, giving rise to the concept of "hole conduction" and treatment of the vacancy as a unit positive charge.

2. Semiconductors

A semiconductor is often defined as a solid possessing electrical conductivity intermediate between that of metals and insulators. Characteristic conductivities near room temperature may be summarized:

metals	10^{4} to 10^{6} $ohm^{-1}cm.^{-1}$
semiconductors	10^{-9} to 10^{3}
insulators	10^{-22} to 10^{-10}

This definition is often restricted to include only electronic conduction and to eliminate conduction by ions. Semiconductors show a negative temperature coefficient of resistance.

Fundamental features for distinguishing metals, semiconductors and insulators can also be made in terms of energy bands. In insulators the valence band is full and the conduction band is empty; there is no net motion of charge when an electric field is applied. In metals either the valence band is only partially filled or a filled band overlaps an empty band and electrons are free to move in an applied field. There are many such free electrons and large conductivities result. Semiconductors near the absolute zero of temperature are insulators, but at higher temperatures finite but limited (equilibrium) concentrations of free electrons

and holes are present and these give rise to an intrinsic, intermediate electrical conductivity. These electrons are thermally excited from the valence band across the forbidden energy gap to the conduction band; the electrons in the conduction band and the holes simultaneously produced in the valence band give rise to the electrical conductivity. The temperature necessary to produce appreciable intrinsic semiconductivity depends on the width of the forbidden gap; an insulator can become an intrinsic semiconductor at sufficiently high temperature.

Imperfections in the crystal lattice of a semiconductor are responsible for many of its unique electrical properties. These imperfections may be foreign atoms that are substitutionally or interstitially incorporated into the crystal, deviations from stoichiometry, or physical defects in the lattice (dislocations and vacancies). Only those imperfections of a chemical nature will be considered here.

Metallic oxides are well-known semiconductors. Their electronic properties may be controlled either by regulating their stoichiometry, or by incorporating impurity foreign atoms into the crystal lattice. Nonstoichiometry can be produced by establishing an equilibrium between the imperfection and a vapor at high temperature and then quenching so that the atomic imperfection is frozen into the crystal. The imperfections may be vacant lattice sites or one component in excess in interstitial sites. Excesses or deficiencies of cations (metal) or anions (oxygen) can be obtained. However, nonstoichiometric crystals are of rather limited applicability as compared to crystals incorporating foreign atoms of deviating valency which control the electrical behavior.

Substitution of appropriate impurity atoms into the host lattice (controlled valency) introduces electrically active centers. This process modifies the semiconductivity of an oxide by substituting a metallic impurity of different valence for a small amount of the normal cation. Stoichiometric, pure oxides have probably rarely been realized and some kind of imperfection has been responsible for the electrical behavior. For such compound semiconductors a high charge-carrier concentration generally exists; this concentration can be varied but the carrier type cannot be changed and, hence, these compounds are known as single-carrier semiconductors.

Stoichiometric, pure nickel oxide of low electrical conductivity is an illustration. In practice nickel oxide is a p-type semiconductor because in thermal equilibrium it contains some Ni^{+++} ions and excess oxygen. The concentration of holes can be increased by incorporating a monovalent ion (e.g., Li^{+} or Ag^{+}) into the lattice for Ni^{++}; this leads to the presence of an equivalence of Ni^{+++} in the lattice in order to preserve electrical neutrality. Electrons can now pass from divalent to trivalent nickel ions, or positive charge in the opposite direction, and conduction by holes is said to occur. The concentration of holes may be decreased by adding a trivalent ion (e.g., Ga^{+++} or Cr^{+++}). However, nickel oxide cannot be converted to an n-type semiconductor.

Analogously, zinc oxide is and remains an n-type semiconductor because it is a metal-excess compound; its free-electron concentration may be modified by incorporating ions of appropriate valence into its lattice.

3. Elemental Germanium

Early investigations of properties of semiconducting solids often employed metallic oxides or sulfides. However, availability of large, nearly perfect single crystals of germanium and silicon, achievement of extreme purity, and control over the addition and distribution of impurities, have been responsible for a tremendous advancement in knowledge of Group IV elemental semiconductors. Now, germanium and silicon are better understood solids than oxides.

Consideration of elemental germanium as a semiconductor is appropriate at this time. Figure 3 is an illustration of impurity semiconduction using germanium as the host crystal. Germanium crystallizes in the diamond-type lattice with each atom tetrahedrally surrounded by four nearest neighbors as a result of hybridization of s and p atomic orbitals to form sp^3 tetrahedrally-directed bonds. Figure 3 depicts this situation in two dimensions with covalent bonding between adjacent germanium atoms. Replacement of a germanium atom by an element of Group V (e.g., arsenic, Figure 3a) produces n-type semiconductivity (negative current carriers); four of the five valence electrons from the arsenic form covalent bonds with adjacent germanium atoms while the fifth electron is only weakly bound to the arsenic and can be removed to large distances easily (ionization energy 0.0127 e.v.).[65] The arsenic is left as an ion of net positive charge upon donating an electron to the conduction band.

If a germanium atom is replaced by an element of Group III (e.g., indium), a deficiency of valence electrons (an excess of holes) will result (Figure 3b). Indium can contribute three electrons to form

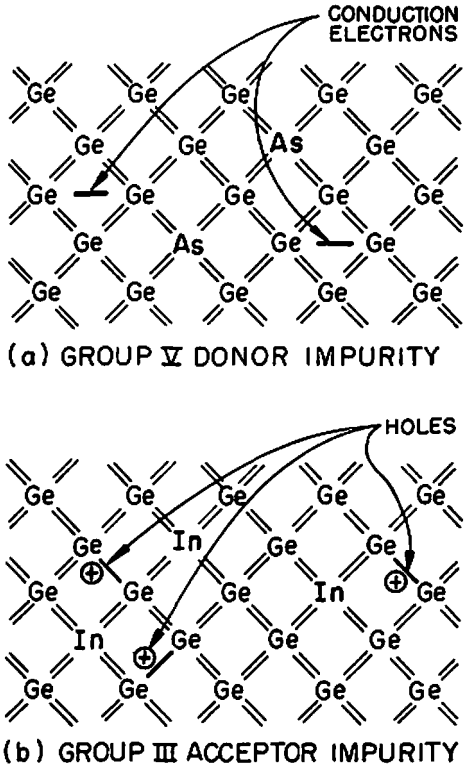

Figure 3. Impurity semiconduction in germanium.

covalent bonds with three adjacent germanium neighbors, but the fourth bond lacks an electron necessary for covalent bond formation. This hole is weakly attracted to the indium but can be ionized away (ionization energy 0.0112 e.v.),[65] leaving the indium with a net negative charge, and producing a hole in the valence band of the germanium. Group III elements are acceptor impurities because when ionized they have accepted electrons; holes, which are positive current carriers, are introduced into the valence band and produce p-type semiconductivity.

Germanium is a two-carrier semiconductor because the type and concentration of electrical charge carriers can be controlled by selection of the appropriate impurity atom. All Group III and V elements are believed to be incorporated substitutionally into the germanium lattice; controlled concentrations from near 10^{13} to about 10^{20} atoms per $cm.^3$ are possible. Their energy levels lie in the forbidden energy gap at localized levels only slightly removed from the bandedges (<0.013 e.v.),[65] so that even at room temperature, thermal excitation energy is sufficient to ionize them.

The electrical behavior just discussed is called "extrinsic" because it depends on the concentration of imperfections in the lattice. "Intrinsic" semiconduction is an intrinsic property of the solid and occurs when thermal excitation frees an electron from the interatomic bond (Figure 2); mobile conduction electrons and holes are created simultaneously in equal numbers. A dynamic equilibrium exists in which generation and recombination of electron-hole pairs takes place. This equilibrium, as is true for other equilibria concerning defects in solids,

can be treated by the law of mass action. For a given solid the product of electron and hole concentrations is a function only of temperature:

$$K = np \tag{1}$$

where K is the equilibrium constant, n is the electron concentration and p is the hole concentration. For intrinsic conditions, $n = p$; thus:

$$K = n_i^2 \tag{2}$$

where n_i is the intrinsic electron concentration at a given temperature.

Equation (1) applies not only when electrons and holes are in equal concentration, but also to conditions when they are not equal. As has been discussed, this situation may result from incorporation of certain foreign atoms into substitutional positions of the crystal (extrinsic semiconduction), in which case n or p are changed from their values under intrinsic conditions. However, their product, as shown in Equation (1), must remain constant; one of these quantities will be in major concentration, the other, in minor concentration. When the concentration of majority carriers is several orders of magnitude larger than the concentration of minority carriers, in effect, a single-carrier system is operating.

4. The Fermi Energy

Fermi-Dirac statistics describe the distribution of free electrons in a system:

$$f(E) = \frac{1}{1 + e^{(E-E_F)/kT}} \tag{3}$$

where $f(E)$ is the probability that a state of energy E is occupied, E_F is a parameter known as the Fermi energy, k is Boltzmann's constant, and T is the absolute temperature.

Figure 4 represents the Fermi-Dirac distribution of completely free (conduction) electrons. Figure 4a plots the probability of occupation as a function of energy for absolute zero and for higher temperatures. At absolute zero the electrons occupy the lowest energy states; E_F is the energy of the highest occupied state. At higher temperatures electrons in the neighborhood of the Fermi level become distributed in states approximately kT above and below the Fermi level. The Fermi energy then becomes the energy for which the probability of occupation is 1/2. Figure 4b represents the distribution of energy given by the Fermi-Dirac theory. At the absolute zero of temperature all states are occupied up to the Fermi level but for $E>E_F$, all states are empty. At higher temperatures, the distribution is rounded off and as many states above E_F are occupied as are unoccupied below it; a more nearly Maxwellian distribution results.

In an intrinsic semiconductor at $T = 0$, the Fermi level is exactly halfway between the valence band and the conduction band; at higher temperatures its position is nearly the same. It is desirable, however, to determine the variation in position of the Fermi level under extrinsic conditions. This can be done by considering the concentration of free charge carriers under equilibrium conditions:

$$n \simeq N_C e^{-(E_C-E_F)/kT} \tag{4}$$

where

$$N_C = 2\left[\frac{2\pi m_n^* kT}{h^2}\right]^{3/2}, \tag{5}$$

n is the concentration of free electrons, N_C is known as the effective

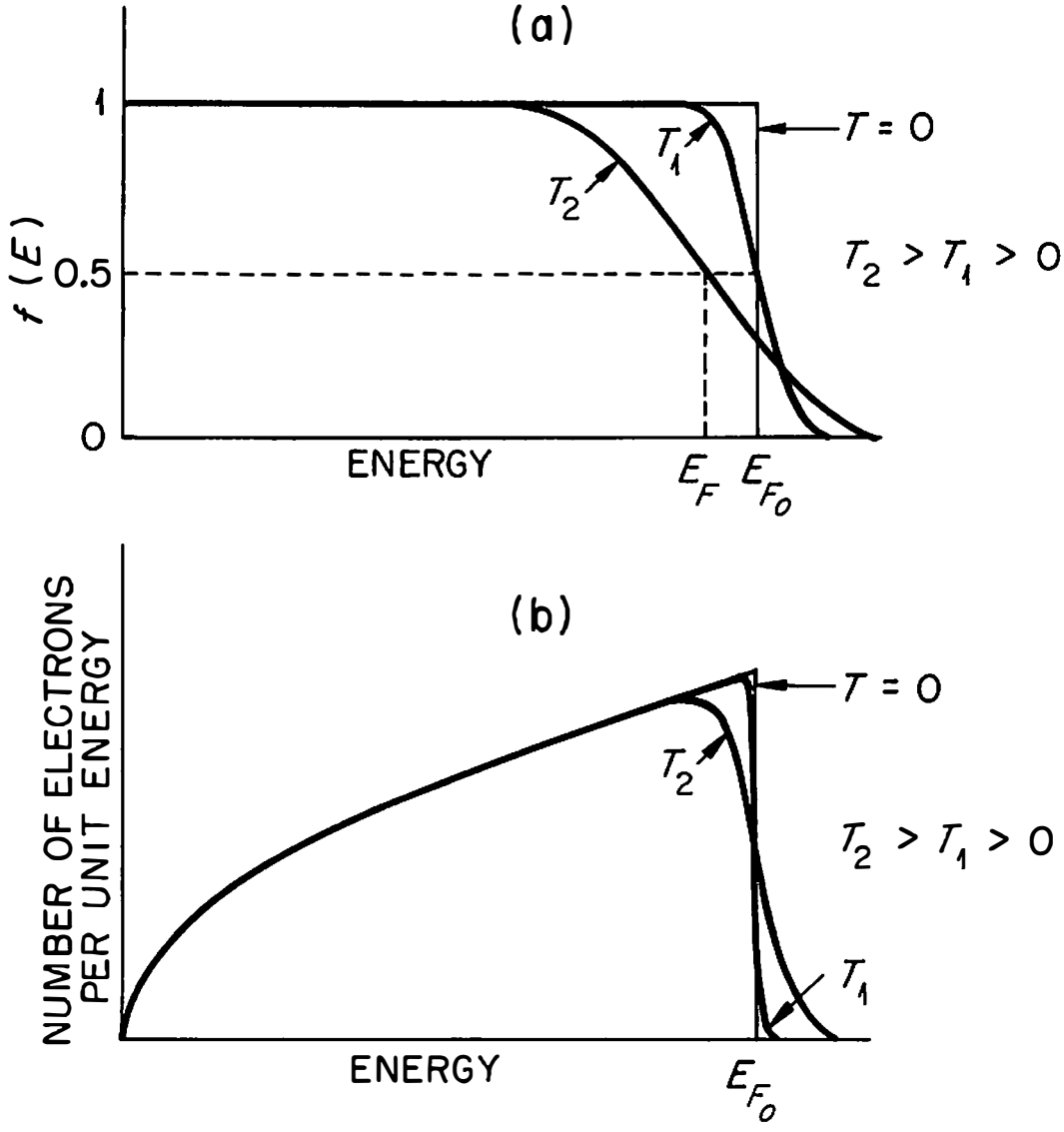

Figure 4. Fermi-Dirac distribution of conduction electrons.

density of states in the conduction band, k is Boltzmann's constant, T is the absolute temperature, h is Planck's constant, E_C is the energy (referred to an arbitrary zero) corresponding to the bottom of the conduction band, E_F is the Fermi energy, m_n^* is the effective mass of the electron and is a function of the energy. A similar equation for positive holes may be written:

$$p \simeq N_V e^{-(E_F-E_V)/kT} \tag{6}$$

where

$$N_V = 2\left[\frac{2\pi m_p^* kT}{h^2}\right]^{3/2}, \tag{7}$$

and in which p is the concentration of positive holes, N_V is the effective density of states in the valence band, m_p^* is the effective mass of positive holes, and E_V is the energy (referred to an arbitrary zero) corresponding to the top of the valence band.

The product of the concentrations of free charge carriers becomes:

$$np = N_C N_V e^{-E_G/kT} \tag{8}$$

where

$$E_G = E_C - E_V \tag{9}$$

and E_G is the width of the forbidden gap. For intrinsic conditions $n = p = n_i$ so that $n_i^2 = np$ and

$$n_i = (N_C N_V)^{1/2} e^{-E_G/2kT} . \tag{10}$$

At any particular temperature for a given semiconductor:

$$n_i^2 = np = \text{constant}.$$

This is the law of mass action, expressed in Equation (2).

Equations (4) and (6) relate the position of the Fermi level and the concentration of free-charge carriers. Under extrinsic conditions

the concentration of free carriers which originate from impurity centers is normally far greater than the concentration of intrinsic carriers. Under such conditions the effective concentration of free carriers is equal to the concentration of ionized impurity atoms. If the impurity atoms are easily ionized, as the Group III and V atoms in germanium are, the concentration of free carriers is equal to the concentration of impurity atoms:

$$n \simeq N_{D^+} \simeq N_D \tag{11}$$

$$p \simeq N_{A^-} \simeq N_A \tag{12}$$

where N_D and N_A are the total density of impurity donors and acceptors, respectively, and N_{D^+} and N_{A^-} are the density of ionized donors and acceptors. Using these approximations in Equation (4):

$$N_D \simeq n \simeq N_C e^{-(E_C-E_F)/kT} = \text{constant} \times T^{3/2} \times e^{-(E_C-E_F)/kT}. \tag{13}$$

The position of the Fermi level depends upon the temperature and the carrier concentration. At constant temperature and with essentially only singly-ionized impurity donors:

$$E_F \propto \ln N_D \tag{14}$$

From Equations (6) and (12) similarly, at constant temperature:

$$E_F \propto -\ln N_A \tag{15}$$

Figure 5 shows the dependence of the Fermi level in germanium upon temperature and carrier density.[66]

Although "Fermi level" is the term used in semiconductor physics, it is identical with the electrochemical potential (μ, the partial molar free energy per electron):[67]

$$\mu = \left(\frac{\partial F}{\partial N}\right)_{P,T} \tag{16}$$

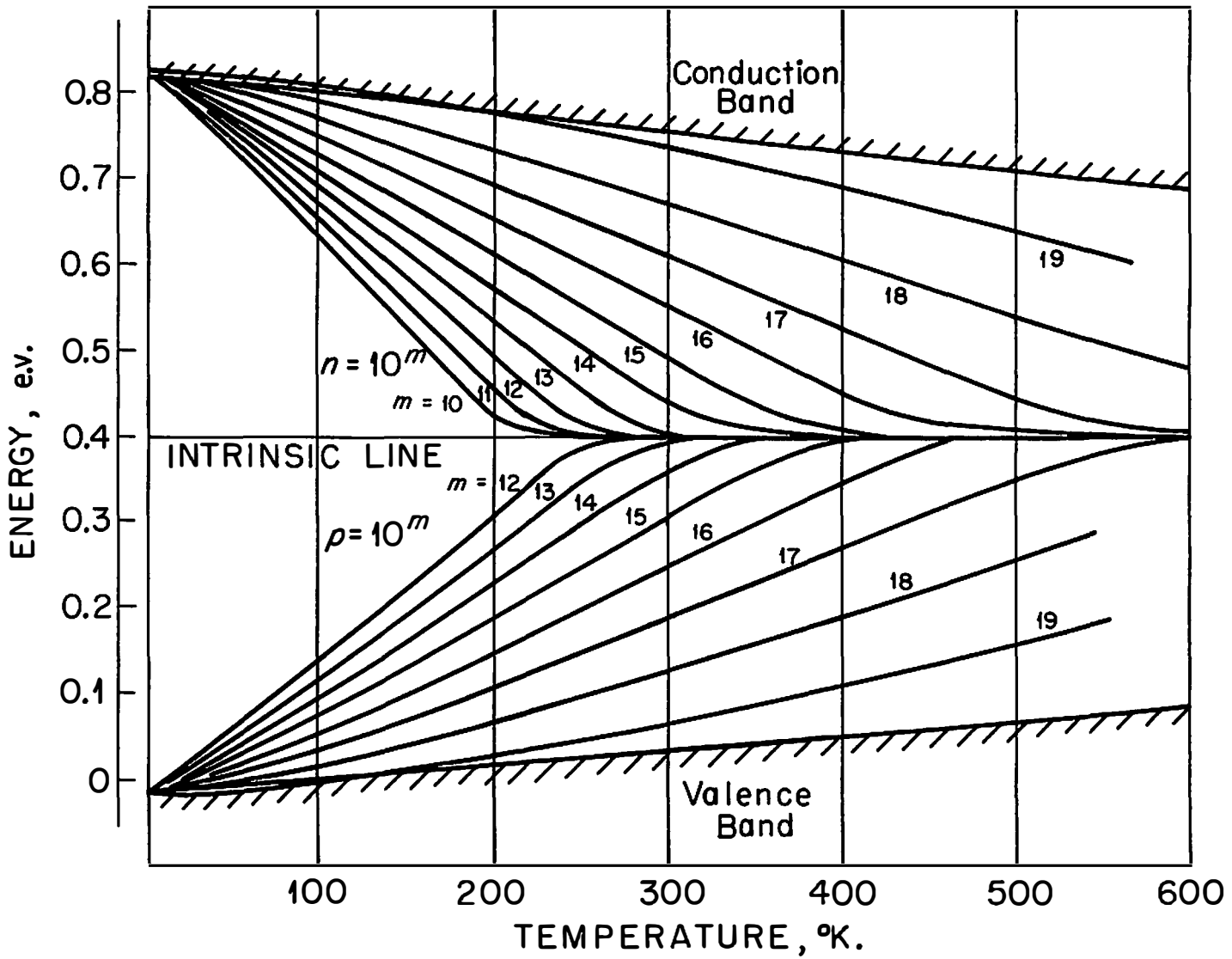

Figure 5. Position of Fermi level in germanium.

where μ is the electrochemical potential, F is the free energy, and N is the total number of particles. In these terms, if two systems come to equilibrium, their electrochemical potentials become equal, i.e., they exchange electrons until their Fermi levels are equal by transferring electrons from filled states of higher energy in one system to lower-lying empty states in the other system.

5. Semiconductor Surfaces

The preceding sections have been concerned with bulk effects in semiconductors. The orderly arrangement of atoms in the bulk crystal lattice suddenly terminates at the surface, however, and this may give rise to surface energy states (Tamm states). Furthermore, molecules of gases may be adsorbed, which may be accompanied by electron transfer. Such processes may result in differences in surface and bulk properties, so that the Fermi level at the surface may not be determined entirely by the bulk impurity density but partly by the charge density at the surface.

Electron exchange, or localization of charge carriers at the phase interface, has been clearly shown to occur during chemisorption through measurements of electrical conductivity of semiconductors during exposure to gases. The relative electronic chemical potentials of the chemisorbing gas and solid determine whether electrons are provided or accepted by the solid. However, in contrast to metals, the positive or negative charge acquired by the semiconductor in this process is not localized directly at the surface, but extends a finite distance into the crystal because of the much lower concentration of charge carriers in the semiconductor than in metals. An electronic boundary layer is thus produced at the surface

of the semiconductor, and may impede electronic communication between the bulk crystal and the surface.

Figure 6 illustrates the formation of a boundary layer due to anionic chemisorption on an n-type semiconductor. The process is analogous to that which takes place at the contact of a metal and a semiconductor; the initial difference in the free energy of the electrons in the two solids (Fermi levels) produces a flow of electrons across the contact until the Fermi levels are equal (equilibrium). In Figure 6 the energy change associated with the transfer of an electron from the semiconductor to the first adatom will be $(\alpha - \phi)q$, where α is the electron affinity of the atom, ϕ is the work function of the semiconductor, and q is the electronic charge. Exothermic donation will continue until the potential energy of electrons in the adsorbate becomes equal to the potential energy of electrons in the semiconductor (the Fermi level). During this chemisorptive process, electrons from impurity levels deeper in the solid are required and a space charge builds up in the boundary layer. This results in a modification in the potential energy of electrons in the solid, and a potential barrier must be overcome to transfer electrons from semiconductor to adsorbate. Treatment of chemisorption on semiconductors as an electronic boundary layer problem has been able to account for many phenomena which have been observed experimentally.

Chemisorption beyond the equilibrium point is not possible because the process no longer leads to a decrease in the free energy. At equilibrium the potential barrier is represented by V in Figure 6, and N^- represents the adsorbed atoms. A number of electrons have been transferred

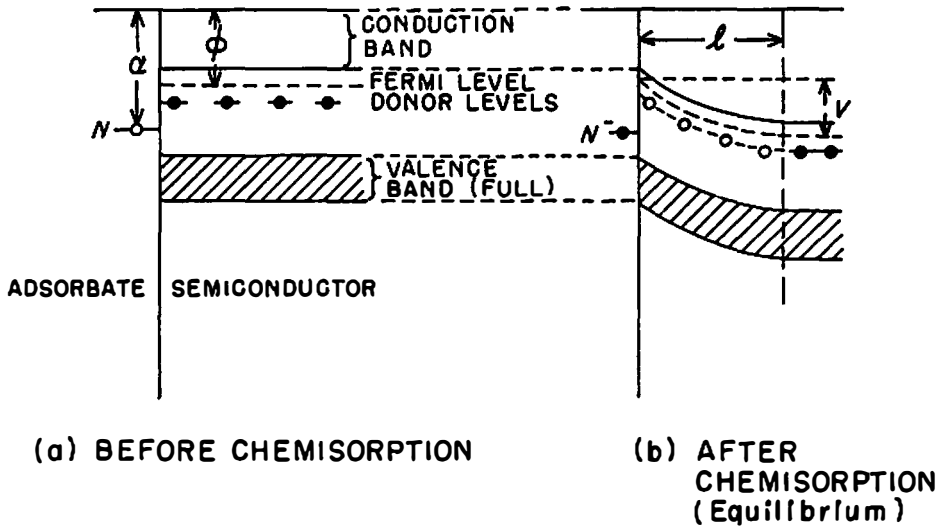

Figure 6. Boundary layer formation. Diagrammatic representation of anionic chemisorption on an *n*-type semiconductor.

from the semiconductor to the substrate, causing a depletion of carriers in the boundary layer to a depth ℓ.

The thickness of this boundary layer is determined in part by the impurity density. For depletive chemisorption as just described this thickness is inversely proportional to the square root of the impurity concentration. For highly pure semiconductors (i.e., low concentrations of impurity atoms) the boundary layer can be quite thick and surface properties can assume great importance. However, for high carrier concentrations ($>10^{18}$ atoms/cm.^{3}) in the bulk, the boundary layer is quite thin (<100 Å.) and changes in the Fermi level in the bulk are expected to produce parallel changes in the Fermi level at the surface.

Heterogeneous catalysis is now generally conceded to be preceded by chemisorption which implies chemical bonding between adsorbate and solid, so that electron transfer or sharing need be considered. Since the solid must either provide or accept electrons in the chemisorptive process, it seems likely that the electronic structure of the solid would influence its catalytic activity. The research described in this thesis used as a catalyst a semiconductor whose Fermi level in the bulk solid could be varied appropriately throughout the forbidden energy gap; this requires relatively high concentrations of charge carriers in the solid (but still only 25 to 5000 p.p.m. impurities). An important consequence of this chemical doping is that the influence of surface properties is most likely minimized as described above. Under such conditions electronic events on the surface (e.g., chemisorption and catalytic activity) are apt to be closely associated with bulk electronic properties.

CHAPTER II

EXPERIMENTAL

The work on which this thesis is based was part of a more general investigation being carried out at the Oak Ridge National Laboratory, to study the effect of high-energy radiations on solid catalysts. It was required, therefore, that the apparatus and techniques be adapted to this broader problem.

In general, reactant gases were introduced into a reaction vessel containing the catalyst, and the chemical reaction permitted to proceed partly to completion at constant temperature; the product gases were then removed and identified, and their concentration determined. The hydrogen-deuterium exchange and the decomposition of formic acid vapor were the two test reactions employed. Samples of chemically-doped elemental germanium were used as catalysts.

A. Vacuum System

A conventional vacuum system was constructed using 10-mm. O.D. Pyrex tubing. Eck and Krebs vacuum stopcocks, which were lubricated with "Apiezon-N" grease, were used. Figure 7 is a schematic diagram of the system used for studying the hydrogen-deuterium exchange. Not illustrated, but indicated at (R), is a second reaction vessel system which was employed in the experiments on the decomposition of formic acid; it is essentially identical to (N).

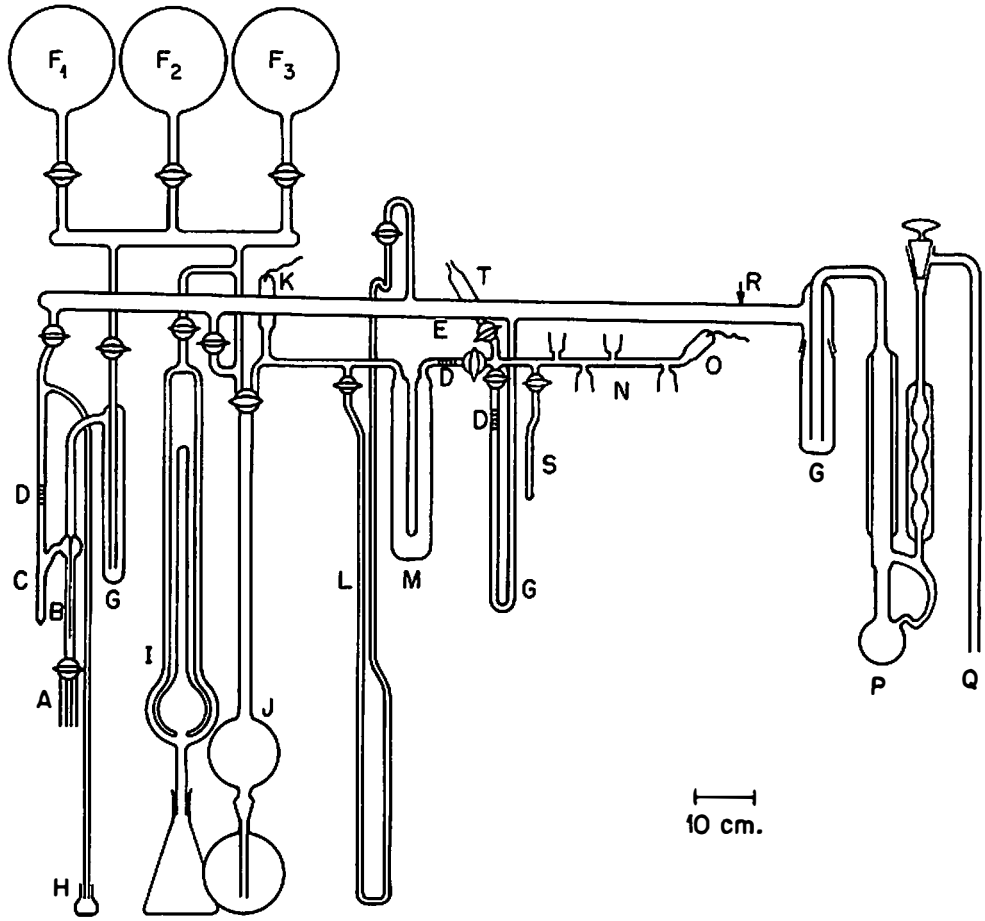

A. HYDROGEN AND DEUTERIUM INLET
B. PALLADIUM THIMBLE
C. PALLADIUM THIMBLE BYPASS
D. DENTAL GOLD FOIL TRAPS
E. VACUUM MANIFOLD, 22-mm. O.D. PYREX
F. GAS RESERVOIRS, 3 liter
G. LIQUID-NITROGEN TRAP
H. MERCURY PRESSURE RELIEF
I. McLEOD GAUGE
J. TÖPLER PUMP
K. PIRANI GAUGE
L. MERCURY MANOMETER
M. COPPER-FILLED LIQUID-NITROGEN TRAP
N. REACTION VESSEL SYSTEM
O. THERMISTOR PRESSURE GAUGE
P. MERCURY DIFFUSION PUMP
Q. TO FORE PUMP
R. TO FORMIC ACID SYSTEM
S. LIQUID-NITROGEN COLD FINGER
T. AIR-INLET DRYING TUBE

Figure 7. Schematic diagram of vacuum system.

It was considered essential to exclude mercury vapor from certain parts of the system, particularly the palladium thimble, and the reaction vessel systems (N) and (R). This was accomplished by means of dental gold foil. The reaction vessel systems were protected with liquid-nitrogen traps as well, so that the catalysts would be kept as free as possible from contamination.

Gas pressures in the system could be monitored as desired. A thermistor gauge, connected to the interspace of (N), and a Pirani gauge connected similarly to (R), monitored the extent of evacuation of the reaction vessel interspace. These gauges were calibrated with the McLeod gauge.

B. Reaction Vessels

Figure 8a shows the quartz reaction vessel which contains a bubble-type break seal at one end and two entry tubes at the other. After fabrication, the vessels were flushed with 6 M. nitric acid, rinsed thoroughly with distilled water, and dried.

The powdered catalyst was added to the vessel through tube (C). Quartz-to-Pyrex graded seals with 2-mm. vacuum stopcocks were sealed onto (C) and (C'). After treatment of the catalyst at elevated temperatures with hydrogen sweeping through the vessel via tubes (C) and (C'), the latter tube was removed at the constriction (DD), leaving the reaction vessel as shown in Figure 8b.

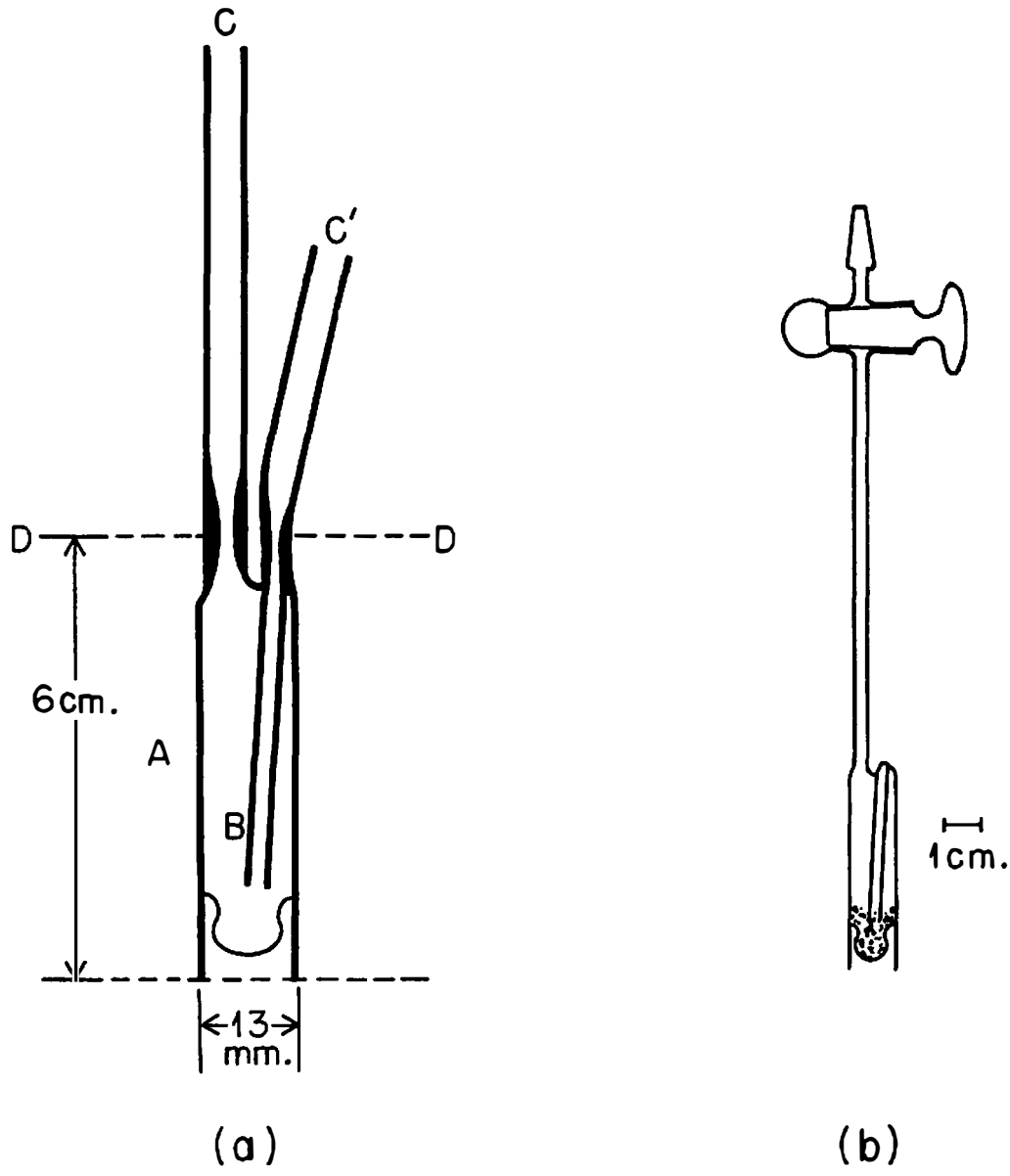

Figure 8. Quartz reaction vessel.

The volume of the main body of the reaction vessel (A in Figure 8) was approximately 3 ml. with another approximately 3 ml. in dead space between (DD) and the stopcock.

C. Germanium Catalysts

Specimens of germanium were obtained from the Bell Telephone Laboratories, Incorporated, Murray Hill, New Jersey, and from the Solid State Division of the Oak Ridge National Laboratory. These samples were sections either of single crystals or of polycrystalline buttons. Both sources supplied information on the impurity content of the materials.

The samples were washed with acetone, and etched for approximately two minutes in CP-8 which is a mixture of concentrated nitric, hydrofluoric and acetic acids in the volume ratio 5:3:3.[68] After thorough rinsing with distilled water and drying, each sample, wrapped in paper, was fractured into smaller pieces by striking it sharply with a hammer. These smaller fragments were crushed and then mechanically ground with an agate mortar and pestle for one hour.

Before using these powders as catalysts, they were treated in flowing hydrogen at high temperature in order to remove any oxygen or oxide film from the surface. The reduction of germanium dioxide by hydrogen at elevated temperatures is a well-known method for the preparation of metallic germanium.[52, 69, 70] The amount of germanium desired for use as the catalyst was weighed into the reaction vessel as described in the previous section. The reaction vessel was centered in a 12-in. horizontal

tube furnace whose temperature was controlled by means of a Wheelco controller which was actuated by a quartz-enclosed thermocouple adjacent to the reaction vessel. The temperature was brought slowly to 675° to 700° and maintained there for approximately two hours while purified hydrogen was slowly passed over the germanium. Matheson Electrolytic, "Prepurified" hydrogen (99.9 per cent minimum purity and <20 p.p.m. nominal oxygen) was used, and was purified by passage through a Model D "Deoxo" Purifier (Engelhard Industries, Inc.) and a liquid-nitrogen trap. The germanium was permitted to cool in the hydrogen atmosphere.

A very thin, brown to black film formed on the cooler walls of the exit tube during the high-temperature treatment with flowing hydrogen. Although this might have resulted from the deposition of very fine germanium powder transported by the flowing hydrogen, it more likely was the result of condensation of germanium monoxide in cooler parts of the system before reduction was completed, as observed frequently by other investigators.[52, 69] Since the gas-exit tube was no longer required after the hydrogen treatment, it (and, thereby, this film) was removed, and the reaction vessel then contained only the hydrogen-treated germanium powder (Figure 8b).

The surface area of each germanium catalyst was determined from krypton adsorption isotherms at the completion of the catalytic studies. These measurements were performed by the surface area group at the Oak Ridge Gaseous Diffusion Plant.

Table I summarizes pertinent information about the germanium catalysts and the reaction vessels. The weights of the catalysts are the

TABLE I

PROPERTIES OF GERMANIUM CATALYSTS AND REACTION VESSELS

Semiconductor			Catalyst		Reaction Vessel	
Type	Impurity	Concn. atoms/cm.^{3}	Specific Surface Area m.^{2}/g.	Wt., g.	Total Vol., ml.	Code
p	Ga	2×10^{20}	0.152	1.337	7.37	A26
	Al	10^{20}	.102	1.106	5.80	A36
	Al	10^{20}	.080	1.183	6.46	A33
	Ga	4×10^{18}	.170	0.980	6.78	A31
	In	2×10^{18}	.139	1.022	6.13	A35
	Ga	1×10^{15}	.125	1.087	8.00	A23
n	Sb	10^{18}	.106	1.190	6.83	A32
	As	5×10^{18}	.113	1.575	6.22	A34
	As	3×10^{19}	.226	1.310	- [a]	A30
	Sb	10^{20}	.106	1.279	7.58	A25
	Sb	10^{20}	.143	1.393	5.87	A37
-	-	-	-	-	9.90	A0[b]

[a] Vessel accidentally broken; used average volume, 6.77 ml.

[b] Empty quartz reaction vessel.

average of the amount used initially and the amount recovered. This difference varied from 0.00 to 0.12 g.; and generally showed an apparent loss of material. Considering the amount of glass blowing performed after the germanium powder was in place, it is surprising that greater losses did not occur. Volumes of the reaction vessels were obtained from the dimensions of the vessels, and by volumetric measurement at the completion of the catalytic experiments (with germanium removed). The difference between calculated and measured volumes was approximately 2 per cent.

D. Gaseous Reactants

1. Hydrogen-Deuterium

Hydrogen (Electrolytic, "Prepurified"; the Matheson Company, Inc.) and deuterium (Stuart Oxygen Co.) were purified separately but identically by passage through a heated palladium thimble.

As shown in Figure 7, gas from the cylinder entered the vacuum system at (A), and was filtered by the palladium thimble (heated to about 315° to 335°) into the reservoir (F) at the rate of approximately 1 mm. per minute. After purification of one gas by this procedure, the palladium thimble was thoroughly flushed with the other gas before purification of it was started. Each gas was stored separately in one of the reservoirs (F_1, F_2) at a pressure of 55 to 65 cm.

Purity of these gases was determined by mass spectrometric analysis with results shown in Table II. Equal amounts of hydrogen and deuterium were mixed and stored in the third reservoir (F_3), and used in the exchange studies.

TABLE II

MASS SPECTROMETRIC ANALYSIS OF HYDROGEN AND DEUTERIUM GASES

Mass	Species	Per Cent[a] Cylinder Hydrogen[b]	"Deoxo" Hydrogen[c]	Pd Hydrogen[d]	Pd Deuterium[d]	Exchange Gas[e] (1)	(2)
2	H_2	99.0	99.2	95.3	0.6	52.4	49.7
3	HD	ND	ND	3.5	5.5	2.7	3.3
4	D_2	ND	ND	0.2	93.1	44.9	46.8
28	N_2	1.0	0.8	1.0	0.8	0.08	0.15
32	O_2	ND	ND	ND	ND	0.02	-
40	A	ND	ND	ND	ND	-	-

[a] ND: not detected, probably <0.06 per cent.

[b] Matheson Company, Inc., "Prepurified", Electrolytic, Cylinder.

[c] Hydrogen from (b) through "Deoxo" Purifier.

[d] Hydrogen from (c) or cylinder deuterium (Stuart Oxygen Co.) through heated palladium thimble.

[e] Typical analysis after mixing palladium-filtered gases.
(1) Analysis A-134-5, 6-25-58.
(2) Analysis F-50-0, 8-31-60.

2. Formic Acid

Formic acid was freed from water by two different methods.

In the first method, about 38 g. of 98+ per cent formic acid (Eastman Kodak Co.) was shaken with about 3 g. of pulverized boric oxide and let remain in contact approximately 68 hours.[71, 72] During this time, the solid became quite gelatinous; the proportions used should have been sufficient to remove the water present.[73] The liquid was distilled *in vacuo* into a Pyrex reservoir connected to the vacuum system. The first portion of distillate was discarded; only about 18 ml. of the 30 ml. of formic acid originally used was collected. Most of the experimental data on formic acid decomposition were obtained using this material (B_2O_3-dried).

In the second method, Baker and Adamson, Reagent Grade, 88-90 per cent formic acid (750 ml.) was fractionated in a 12-ft. Vigreux column. The first fraction of distillate (about 100 ml.) contained low-boiling contaminants and was discarded. The succeeding two fractions of approximately 125 ml. each were collected at 100.8° and should have consisted of pure, dry formic acid since the distillation was from the formic acid side of the formic acid-water azeotrope (77.5 per cent formic acid).[74] The refractive index of the liquid, determined with a Bausch and Lomb refractometer (Abbe-56 Model), was n_D^{24} 1.3693. Literature values are: b.p. 100.75°,[74] n_D^{20} 1.3710[75] with temperature coefficient -0.00038 per degree,[76] yielding n_D^{24} 1.3695. A portion of this acid was transferred to a Pyrex reservoir which was then connected to the vacuum system.

When not in use, the formic acid was frozen to reduce thermal decomposition; it supercooled at least 8° to 10°.[77] The temperature of

melting of the acid was approximately 8.2 ± 0.4°; recent literature values are 8.1°[75] and 8.4°.[76] The acid was kept in the dark to minimize photochemical decomposition.

E. Experimental Procedure

A batch procedure was used first to investigate the hydrogen-deuterium exchange and then the formic acid decomposition on the same catalyst. The procedures in the exchange and decomposition experiments were identical except for the method of introducing the reactants into the reaction vessels.

Reaction vessels without germanium, but otherwise identical, were used to provide background corrections for the exchange and decomposition reactions.

1. Hydrogen-Deuterium Exchange

The reaction vessel containing the catalyst (Figure 8b) was connected to the vacuum system at (N) (Figure 7), and the interspace was evacuated until a pressure of at least 0.5 micron could be maintained without pumping and without the use of a liquid-nitrogen trap. The 1:1 hydrogen-deuterium exchange mixture was admitted to the evacuated interspace and (previously) evacuated reaction vessel from the Töpler pump, which had been filled with the gas mixture from (F_3). This exchange gas mixture passed through the copper-filled liquid-nitrogen trap and dental gold foil before reaching the catalyst. The pressure could be adjusted by means of the Töpler pump and was determined with the mercury manometer. A pressure of approximately 40 mm. was used in each experiment.

The reaction vessel was then removed from the vacuum system by allowing air to enter (N) through the air-inlet tube filled with anhydrous magnesium perchlorate. The exchange was carried out at constant temperature in the range 100° to 400° by immersing the reaction vessel (the bottom 6 cm. to point (DD) in Figure 8a) in a bath maintained at the desired temperature. The stopcock of the reaction vessel was kept cool by blowing air across it. The baths used mineral oil, silicone oil 550, or a molten salt eutectic mixture (56 per cent potassium nitrate, 14 per cent sodium nitrate, and 30 per cent lithium nitrate, m.p. 120°)[78] as liquids. The temperature was set by adjusting the current to electric resistance heating mantles ("Glas-Col") surrounding the baths. The liquids were stirred rapidly with magnetic stirrers. Temperatures were measured with mercury-in-glass thermometers; in the case of the fused salt bath, the thermometer was immersed in a narrow well containing silicone oil as a heat transfer fluid, since the melt attacked the glass of the thermometer. Temperature control was generally better than ±1° for several hours and ±3° for runs requiring several days.

The exchange mixture was sampled after reaction by returning the vessel to the vacuum system (N), evacuating the interspace, and expanding the gases into an evacuated sample bulb of about 60 ml. capacity. After pumping out the reaction vessel and interspace, the system was ready for introduction of fresh reactants for the next experiment.

2. Formic Acid Decomposition

Experiments on the catalytic decomposition of formic acid used the system sealed to the vacuum manifold at (R). This system was a counterpart

of (N), and consisted of liquid-nitrogen and dental gold foil traps, standard taper joints to accommodate the reaction vessels, a "Drierite"-filled air-inlet tube, formic acid reservoirs isolated by vacuum stopcocks, and a Pirani gauge with stopcock so it could be separated from the system.

In these experiments, the formic acid reservoir was maintained at a temperature which gave the desired vapor pressure of formic acid. The temperature or pressure was determined from the equation:[77]

$$\log P = 7.8584 - \frac{1860}{T} \qquad (17)$$

where P is the vapor pressure in mm. and T is the absolute temperature. The vapor phase of the formic acid reservoir, and the bore of the reservoir stopcock, were purged of possible volatile decomposition products by expanding the vapor repeatedly into the evacuated interspace and pumping it away each time. The purity of the vapor was determined manometrically and found to be better than 99.7 per cent formic acid; carbon monoxide was detected in the vapor by gas chromatography.

The reaction vessel was immersed in a hot water bath (55-60°) during loading so that its temperature was somewhat higher than that of the reservoir and connecting tubing. This procedure limited the amount of formic acid introduced into the reaction vessel, and prevented condensation of formic acid on the cooler walls near the stopcock when the vessel was heated during reaction. Formic acid pressures were usually 42 ± 2 mm.

Sampling of the reaction vessels was generally the same in the experiments with formic acid as it was in the hydrogen-deuterium experiments.

Formic acid is strongly adsorbed on glass at room temperature and desorbs only slowly, even with pumping and liquid-nitrogen traps; leak

up to pressures of several microns was observed even several hours after exposure of the system to formic acid vapor.

F. Analyses

1. Hydrogen-Deuterium Exchange

Analysis in the exchange experiments was by mass spectrometry and was carried out by the Special Testing Department, Isotope Analysis Section, Y-12 Plant, Oak Ridge. A 6-in. radius, 60°, Nier type, gas mass spectrometer was employed. Relative abundances of masses 2, 3 and 4 were determined and yielded the per cent hydrogen, hydrogen deuteride, and deuterium, respectively, in the sample. The abundance of mass 28 (nitrogen) monitored the leakage of air into the system, and was always very small.

Background corrections were obtained by analyzing samples of the original exchange mixture. The unreacted mixture gave a D/H ratio of 1.03 ± 0.08 and showed the presence of 3.0 ± 0.4 per cent hydrogen deuteride, which probably arose from exchange of hydrogen with deuterium in the mass spectrometer.

The reliability of these analyses was determined by comparing results for duplicate samples analyzed a week apart as shown in Table III. Assuming that the precision of the analyses was constant over the range of composition of the samples, a combined estimate of the standard deviation was made.[79] The 95 per cent confidence limits for a mean were ±0.69 per cent hydrogen deuteride.

TABLE III

REPRODUCIBILITY OF MASS ANALYSES

Date of Analysis	Ratio D/H	Per cent HD	Difference	Std. Deviation
3-20-58	0.976	25.40	-0.84	0.594
3-26	.988	24.56		
3-20	.978	28.78	-0.26	.184
3-27	.970	28.52		
3-24	.982	35.00	+1.04	.735
3-28	.930	36.04		
3-24	1.131	2.00	-0.18	.127
3-31	1.159	1.82		
3-26	0.953	37.02	+0.20	.141
4-2	.965	37.22		
3-31	.796	23.60	-0.04	.028
4-3	.789	23.56		
		Combined standard deviation		0.401

2. Formic Acid Decomposition

Formic acid decomposes by two principal paths:

$$HCOOH \rightarrow CO_2 + H_2 \qquad (18)$$

$$HCOOH \rightarrow CO + H_2O. \qquad (19)$$

Although other reactions are possible, there is an abundance of evidence that these are negligible compared with the dehydrogenation and dehydration reactions shown.[80, 81] The method of analysis, therefore, was designed to determine the rate at which the decomposition took place by each of these two paths. This was accomplished by determining the total amount of decomposition by means of manometric measurements (duplicate analyses agreed to about 5 per cent), and by measurement of the relative proportions of carbon dioxide and carbon monoxide in the decomposition products by means of gas chromatography.

Pressures of total gas and of residual gas noncondensable at -78° were measured with a McLeod gauge in a vacuum system which also contained a Töpler pump and cold finger. The gas sample, which had been removed from the reaction vessel, was transferred by means of the Töpler pump to the McLeod gauge. Care was taken to transfer a sufficiently small amount so that the vapor pressure of formic acid was not exceeded during subsequent operations, i.e., less than 42 mm. (at 25°). After measuring the total pressure of decomposition products and undecomposed reactant, the pressure of gas, noncondensable at -78°, was measured by immersing the cold finger in a dry ice-trichloroethylene bath. Under these circumstances, formic acid and water are condensed from the vapor phase, leaving as gases only carbon dioxide, carbon monoxide, and hydrogen. These

gases were then transferred to a small cell (3.6 $cm.^3$) for chromatographic analysis.

A Perkin-Elmer "Vapor Fractometer" Model 154, employing a thermistor-type katharometer as detector, was used. A 2-m. silica gel column at room temperature with helium as the carrier gas at a flow rate of approximately 95 $cm.^3$/min. gave good resolution of these gases. Under these conditions, the elution peak maxima (in arbitrary units of time) appeared at 1.0 (hydrogen), 1.7 (air), 2.0 (carbon monoxide), and 21.1 (carbon dioxide). The concentration of hydrogen in the helium was so low that the katharometer response to hydrogen was in the same direction as that for carbon monoxide or carbon dioxide.[82] In all cases, the amount of air was very small, and appeared to arise from leaks in the chromatographic system. Calibration curves relating peak heights or areas under the elution curves with concentration of hydrogen, carbon monoxide, or carbon dioxide were obtained using known concentrations of the pure gases.

CHAPTER III

EXPERIMENTAL RESULTS

A. Treatment of Data

1. Hydrogen-Deuterium Exchange

First-order rate constants were calculated for the hydrogen-deuterium exchange on germanium[46] from the mass spectrometric analyses (Appendix I). Some rates of exchange, which were typical of the experimental data for n-type, p-type, and intrinsic germanium, are shown in Figure 9. On surfaces of gallium- and indium-doped germanium these were at least ten times faster than those found for empty reaction vessels. However, n-type and aluminum-doped p-type germanium were much less active catalysts, and exchange occurred predominantly on the quartz surfaces of the reaction vessels at the lower temperatures. Because of different activation energies for exchange on these two surfaces (found to be approximately 9 kcal./mole on quartz and 20 to 30 kcal./mole on n-type germanium), germanium catalysis began to dominate above 230° to 280°. This transition of decomposition on competing catalytic surfaces gave a pronounced nonlinear Arrhenius temperature dependence. Consequently, the rate data were corrected for the exchange occurring on quartz to yield first-order rate constants per unit area of germanium surface. These results were treated by the method of least squares to calculate the constants of the Arrhenius equation (see Section 3, below).

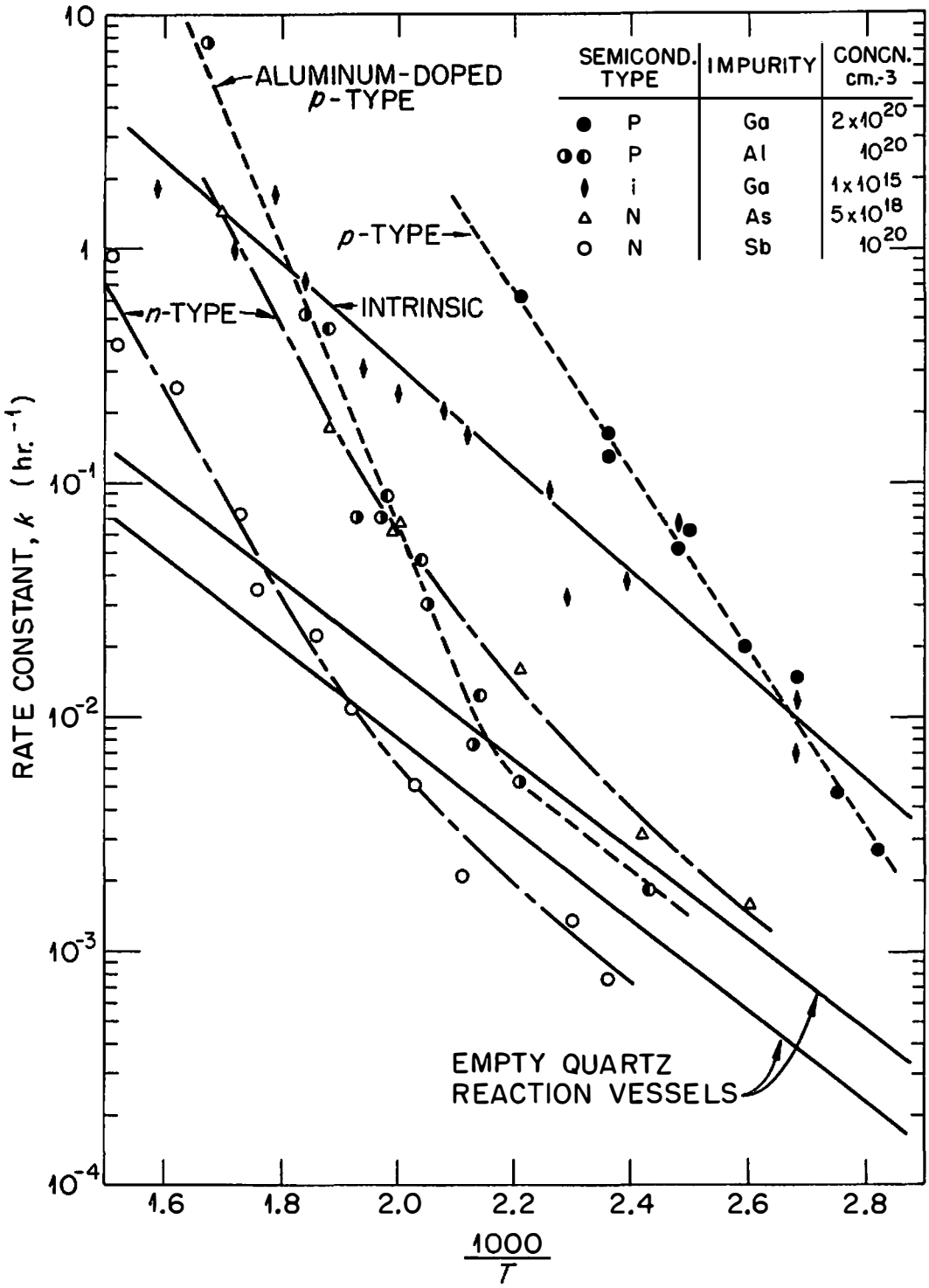

Figure 9. Observed rates of hydrogen-deuterium exchange on chemically-doped germanium.

2. Formic Acid Decomposition

In theory at least, rates of dehydrogenation and dehydration of formic acid can be evaluated from the total rate of decomposition and the relative amounts of carbon dioxide and carbon monoxide in the decomposition products. The method of analysis was based on this premise.

The relative concentrations of carbon monoxide, carbon dioxide, and hydrogen were determined gas chromatographically; the method, which employed a katharometer as detector, was not suited to determine the amount of hydrogen with precision, since the difference in thermal conductivities between hydrogen and the carrier gas (helium) is quite small.

Since dehydrogenation of formic acid produces equal amounts of hydrogen and carbon dioxide, as shown in Equation (18), it was expected that a ratio of H_2/CO_2 close to unity would be observed. Analysis of the chromatograms showed that the ratio H_2/CO_2 was indeed approximately unity (within the estimated limits of error) in the product gases from the empty reaction vessel and from vessels containing n-type germanium. However, the ratio H_2/CO_2 was significantly less than unity in the vapor over p-type germanium, being in the range 0.4 ± 0.2.

This deviation from the stoichiometry expected in the dehydrogenation of formic acid suggested either that the vapor phase did not contain the total amount of hydrogen produced in the dehydrogenation, or that more carbon dioxide was present than was produced solely by dehydrogenation. This last situation might result if formic acid decomposed by another path which would produce carbon dioxide but not hydrogen. Such decomposition might be, for example:

$$2HCOOH \rightarrow CO_2 + H_2O + HCHO \qquad (20)$$

The occurrence of this reaction, together with the dehydrogenation reaction:

$$HCOOH \rightarrow CO_2 + H_2 \qquad (18)$$

would yield a ratio of H_2/CO_2 less than unity.

If these reactions contributed to the decomposition as just postulated, a ratio of H_2/CO_2 near 0.4 would require that an appreciable fraction of the decomposition would have to occur by Equation (20), and, therefore, appreciable amounts of formaldehyde should be present in the product gases. Consequently, an attempt to detect formaldehyde among the gaseous products of the decomposition of formic acid on p-type germanium was undertaken, using mass spectrometry.

The cracking patterns of formic acid and formaldehyde are sufficiently different that the presence of the latter in a mixture of the two should be easily detected by mass analysis. Table IV shows the relative mass abundances for formic acid, formaldehyde, and the decomposition products (A, B, and C for three decomposition runs) of formic acid on indium-doped p-type germanium. The relative abundance at mass 30 may be used to detect the presence of formaldehyde. The mass data for the decomposition samples were normalized at mass 44 (carbon dioxide), and showed only small amounts of mass 30 (formaldehyde) in spite of the fact that the ratios of H_2/CO_2 in these samples (determined chromatographically) were 0.33, 0.25, and 0.52, respectively. Therefore, reaction (20) does not appear to occur as an important path of decomposition of formic acid on p-type germanium.

TABLE IV

MASS SPECTRA OF DECOMPOSITION PRODUCTS OF FORMIC ACID

	Relative Abundance				
			Decomposition Products		
Mass	HCOOH[a]	HCHO[b]	Run A	Run B	Run C
12	0.9	3.3	5.0	4.9	3.1
13	.6	4.3	0.4	0.5	0.1
14	.1	4.4	0.9	0.9	0.4
16	2.3	1.7	8.5	8.0	6.9
18	14.2	-	5.0	3.1	1.4
28	17.4	30.9	15.8	16.0	9.6
29	93.4	100.0	12.4	14.1	4.4
30	1.2	88.5	1.6	1.7	0.6
44	25.9	-	100.0	100.0	100.0
45	77.0	-	1.2	1.3	1.2
46	100.0	-	0.4	0.4	0.4

[a] G. A. Ropp and C. E. Melton, J. Am. Chem. Soc., 80, 3509 (1958).

[b] "Catalog of Mass Spectral Data," Amer. Pet. Inst. Res. Proj. 44, Natl. Bur. Standards, Washington, D. C., Serial No. 84.

This conclusion is entirely in agreement with results reported for other systems.[80, 81] Furthermore, formaldehyde itself may decompose:[81]

$$HCHO \rightarrow CO + H_2 \qquad (21)$$

in which case the over-all products of reaction paths (20) and (21) are exactly those of (18) and (19), that is, dehydrogenation and dehydration.

If carbon dioxide and hydrogen are present only through the process of dehydrogenation, an alternate explanation of the fact that the ratio H_2/CO_2 is less than unity in the vapor over p-type germanium, must be found. This may be the adsorption of hydrogen by p-type germanium, a circumstance that would result in a deficiency of hydrogen in the gaseous decomposition products. This possibility may be explored by comparing the amount of germanium surface available for adsorption with the deficiency of hydrogen in the gas phase. The comparison can be only qualitative, because the ratio H_2/CO_2 is not known accurately. Using average values, about 7 micromoles of formic acid was decomposed according to reaction (18) in these experiments, and, therefore, approximately 3 micromoles of hydrogen and 7 micromoles of carbon dioxide must have been present in the gas phase (assuming no loss of carbon dioxide) in order to obtain a ratio of H_2/CO_2 of about 0.4. Thus, approximately 4 micromoles of hydrogen was missing from the gas and, by the present hypothesis, assumed to be adsorbed by the germanium. Four micromoles represents about 2.4×10^{18} molecules of hydrogen to be adsorbed on a surface of about 0.15 $m.^2$ (equivalent to about 1×10^{18} adsorption sites).

Considering that the above calculation is only an estimate, it seems just possible that sufficient sites on the surface are present to account

for the adsorption of the required amount of hydrogen, and, therefore, for the observed loss of hydrogen from the gas phase. At face value, however, the calculation suggests that hydrogen must be adsorbed in amounts greater than correspond to a monomolecular layer.

Atomic, rather than molecular, hydrogen would probably be involved in such adsorption, since atomic hydrogen is undoubtedly produced when formic acid decomposes directly on surfaces.[83] Experiments by Law and Francois[48] have suggested that germanium adsorbed considerably more atomic hydrogen, which was produced in the decomposition of water on the surface, than molecular hydrogen. This may imply that hydrogen atoms have entered the germanium lattice, a situation that has been discussed by Crawford, Schweinler and Stevens.[84] Green[61] has pointed out that atomic hydrogen which was adsorbed on germanium behaved in an unusual manner based on surface conductivity experiments; he suggested that adsorbed hydrogen atoms were "buried" in the germanium surface and not held to the surface by simple covalent bonds. The association of several hydrogen atoms with each germanium atom seems perfectly admissible when one considers the well-known germanium hydrides, for example, germane (GeH_4) or digermane (Ge_2H_6).

Since no evidence was found for decomposition of formic acid by paths other than dehydrogenation and dehydration, except possibly in very small amounts, and since the disparity in the amounts of hydrogen and carbon dioxide, which were found in the decomposition gases, could be reasonably well explained as due to selective removal of hydrogen by the germanium, these two reactions were considered to be the major paths of

decomposition. Zero-order rate constants (see below) for dehydrogenation (k_{CO_2}) and dehydration (k_{CO}) were calculated from the pressure measurements and the gas chromatographic data, taking into account the dimerization of formic acid vapor and the observed ratio H_2/CO_2, as shown in Appendix II.

These results for the dehydrogenation reaction are shown in Figure 10. Almost all those points representing dehydrogenation on n-type germanium vary within a factor of two (dashed lines in Figure 10) of those for the empty quartz reaction vessel. Since surface reactions are notoriously irreproducible, these results were taken to demonstrate that dehydrogenation on n-type germanium had not occurred; the decomposition that was detected had apparently taken place on the quartz walls of the reaction vessel. Figure 10 shows also that the rate of dehydrogenation on p-type and intrinsic germanium was usually more than ten times faster than that on quartz.

Experiments were undertaken to determine the kinetic behavior of the decomposition of formic acid on p-type germanium; on many surfaces the decomposition is zero order. A reaction is zero order if the rate is independent of the concentrations of the substances involved, that is, the rate of change of the concentrations is constant. The rate expression for the zero-order dehydrogenation of formic acid is:

$$\frac{d[CO_2]}{dt} = k_{CO_2} \tag{22}$$

where t is the time, k_{CO_2} is the rate constant for dehydrogenation, and the brackets mean concentrations. Upon integration, this becomes:

$$[CO_2] = k_{CO_2} t \tag{23}$$

since $[CO_2] = 0$ at $t = 0$.

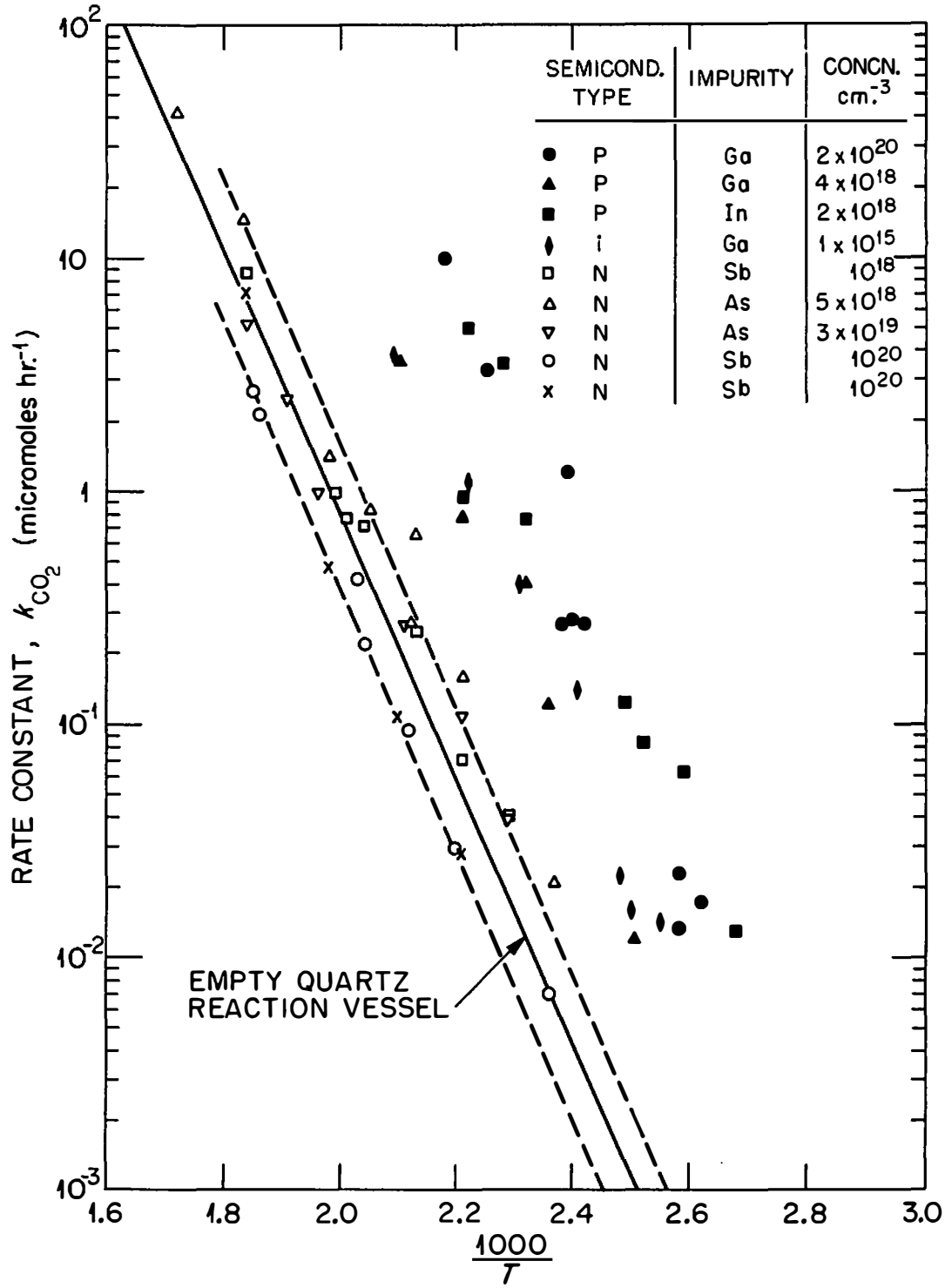

Figure 10. Observed rates of dehydrogenation of formic acid on chemically-doped germanium.

According to Equation (23), a plot of the concentration of carbon dioxide against time should yield a straight line passing through the origin and having a slope equal to k_{CO_2}. Figure 11 is a graphical representation of the data to demonstrate the zero-order kinetics. Both the B_2O_3-dried and the distilled formic acid behaved similarly. Deviations from zero order are seen to occur at about 30 per cent decomposition; the rate data, however, did not fit either first- or second-order rate expressions at all. Similar results have been reported for the decomposition of formic acid on silver.[85]

Many experiments were carried out to decompositions greater than 30 per cent in order to provide amounts of decomposition products sufficient for chromatographic analysis. By using experimental data for decompositions carried out to 80 per cent, an empirical equation was deduced that permitted calculation of rate constants which were consistent with zero-order behavior (Appendix II).

Parenthetically, but of relevance here, the apparatus and techniques which were used in the study of the decomposition of formic acid on germanium were also used for similar studies on copper. The decomposition on copper produced only hydrogen and carbon dioxide in equal amounts as products, was zero order up to at least 70 per cent decomposition, and had an activation energy near 25 kcal./mole. These results are entirely in agreement with those reported in the literature,[86] and, thus, support the validity of the results obtained in experiments with germanium.

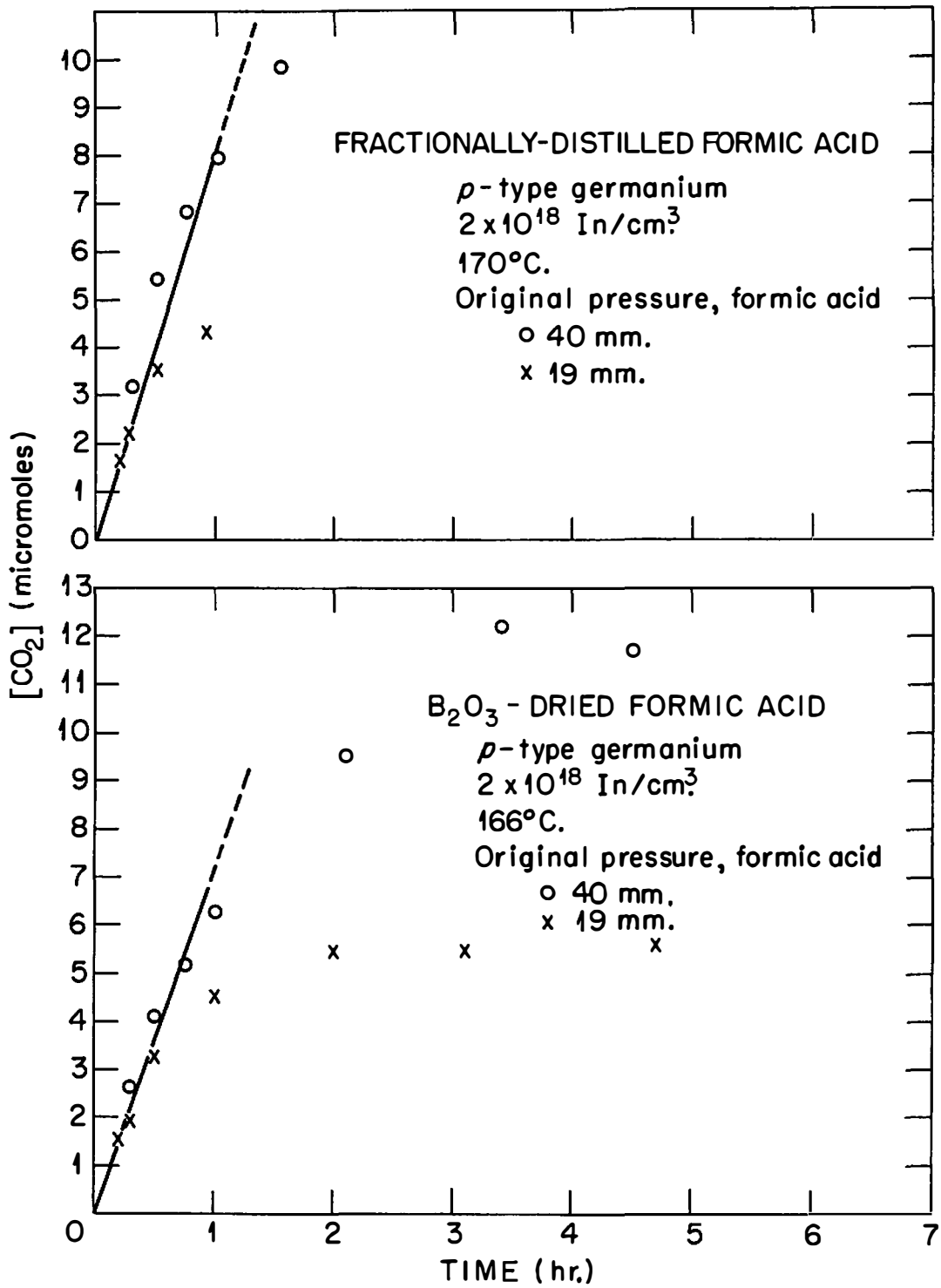

Figure 11. Graphical representation of the decomposition of formic acid on p-type germanium (zero-order reaction).

Dehydration of formic acid on germanium occurred to such a small extent that it was not possible to obtain precise results. Therefore, dehydration was assumed to be zero order, the same as dehydrogenation. The extent of decomposition by dehydration was always less than 19 per cent and no correction for deviations from zero order were believed necessary.

The rates of decomposition were standardized to unit surface area and treated by the method of least squares to calculate constants of the Arrhenius equation (see below).

3. Least-Squares Analysis

The Arrhenius equation may be written:

$$k = A\, e^{-E_a/RT} \tag{24}$$

or

$$\log k = \log A - \frac{E_a}{2.303RT} \tag{25}$$

where k is the specific rate constant, A is the frequency (preexponential) factor, E_a is the apparent activation energy, R is the gas constant, T is the absolute temperature, and the factor 2.303 enters in the conversion from natural to Briggsian logarithms.

The logarithm of the rate constant, log k, is a linear function of $1/T$, as shown in Equation (25). Least-square calculations were used to obtain linear expressions that best fit the experimental data.[87] Frequency factors were obtained directly from these expressions while the slopes of the least-square lines yielded the activation energies. From the variance of each slope, a confidence range on the activation energy

was calculated at the 80 per cent confidence interval. This level was used for the decomposition of formic acid because of the scatter in these data; it was used for the exchange data as well.

B. Results

1. Hydrogen-Deuterium Exchange

Table V summarizes the results for the hydrogen-deuterium exchange, giving the values of the constants in the Arrhenius equation obtained by the method of least squares. Figure 12 is an Arrhenius plot of the results, based on the least-square analyses. The experimental points are not shown in Figure 12 to avoid confusion; their fit to the least-square lines is reflected in the confidence ranges of the activation energies shown in Table V. In Figure 12 the solid line shows results on the intrinsic germanium, the short-dashed lines on p-type germanium, and the long-dashed lines on n-type germanium.

The results for the exchange are also plotted in Figure 13. The three kinetic factors of the Arrhenius equation, i.e., the frequency factor (A), the rate constant at 500°K. (k_{500}), and the apparent activation energy (E_a) are plotted versus the impurity concentration (atoms per $cm.^3$ of germanium). The range in activation energy at the 80 per cent confidence level is indicated by the length of the vertical lines. The dashed curves indicate the trend in kinetic factors of the exchange with changes in the impurity content (semiconductivity) of the solid.

Since the impurity atoms, which were incorporated into the germanium crystals used in this study, all had ionization energies less than

TABLE V

LEAST-SQUARES VALUES FOR THE ARRHENIUS EQUATION

$$\log k = \log A - \frac{E_a}{2.303RT}$$

Semi-cond. Type	Impurity Concn., atoms/cm.^{3}	$H_2 + D_2 \rightleftharpoons 2HD$			$HCOOH \rightarrow CO_2 + H_2$			$HCOOH \rightarrow CO + H_2O$		
		log A[a]	log k_{500}[b]	$(E_a)_{0.8}$[c]	log A[b]	log k_{500}[b]	$(E_a)_{0.8}$[c]	log A[b]	log k_{500}[b]	$(E_a)_{0.8}$[c]
p	2×10^{20} Ga	8.8	1.2	17 ± 1	16.6	3.0	31 ± 2	10.0	1.4	20 ± 2
	10^{20} Al	14.0	-0.3	33 ± 2	16.7	2.9	32 ± 4	13.5	1.4	28 ± 3
	10^{20} Al	13.6	-0.4	32 ± 3	-	-	-	-	-	-
	4×10^{18} Ga	6.4	0.1	14 ± 2	15.3	2.3	30 ± 5	12.2	0.9	26 ± 5
	2×10^{18} In	4.5	-0.1	10 ± 1	16.9	3.6	30 ± 1	11.0	1.1	23 ± 6
i	1×10^{15} Ga	4.8	0.3	10 ± 1	14.2	2.3	27 ± 4	9.5	0.5	21 ± 2
n	10^{18} Sb	11.8	-1.6	31 ± 5	No detectable			9.4	0.3	21 ± 3
	5×10^{18} As	7.1	-0.4	17 ± 1	decomposition			10.1	0.0	23 ± 4
	3×10^{19} As	6.9	-2.3	21 ± 5				8.4	-0.1	20 ± 1
	10^{20} Sb	8.7	-1.9	24 ± 3	$\log k_{500} < 1$			7.2	0.2	16 ± 2
	10^{20} Sb	7.1	-2.2	21 ± 2				12.4	-0.1	29 ± 5
Empty quartz reaction vessel[d]		4.8	0.9	9 ± 1	13.9	2.6	26 ± 1	11.6	1.5	23 ± 4

[a] A and k in units: hr.$^{-1}$ m.$^{-2}$

[b] A and k in units: micromoles hr.$^{-1}$ m.$^{-2}$

[c] E_a in units: kcal./mole

[d] Germanium data corrected for quartz background; relative surface areas, germanium to quartz ~ 100.

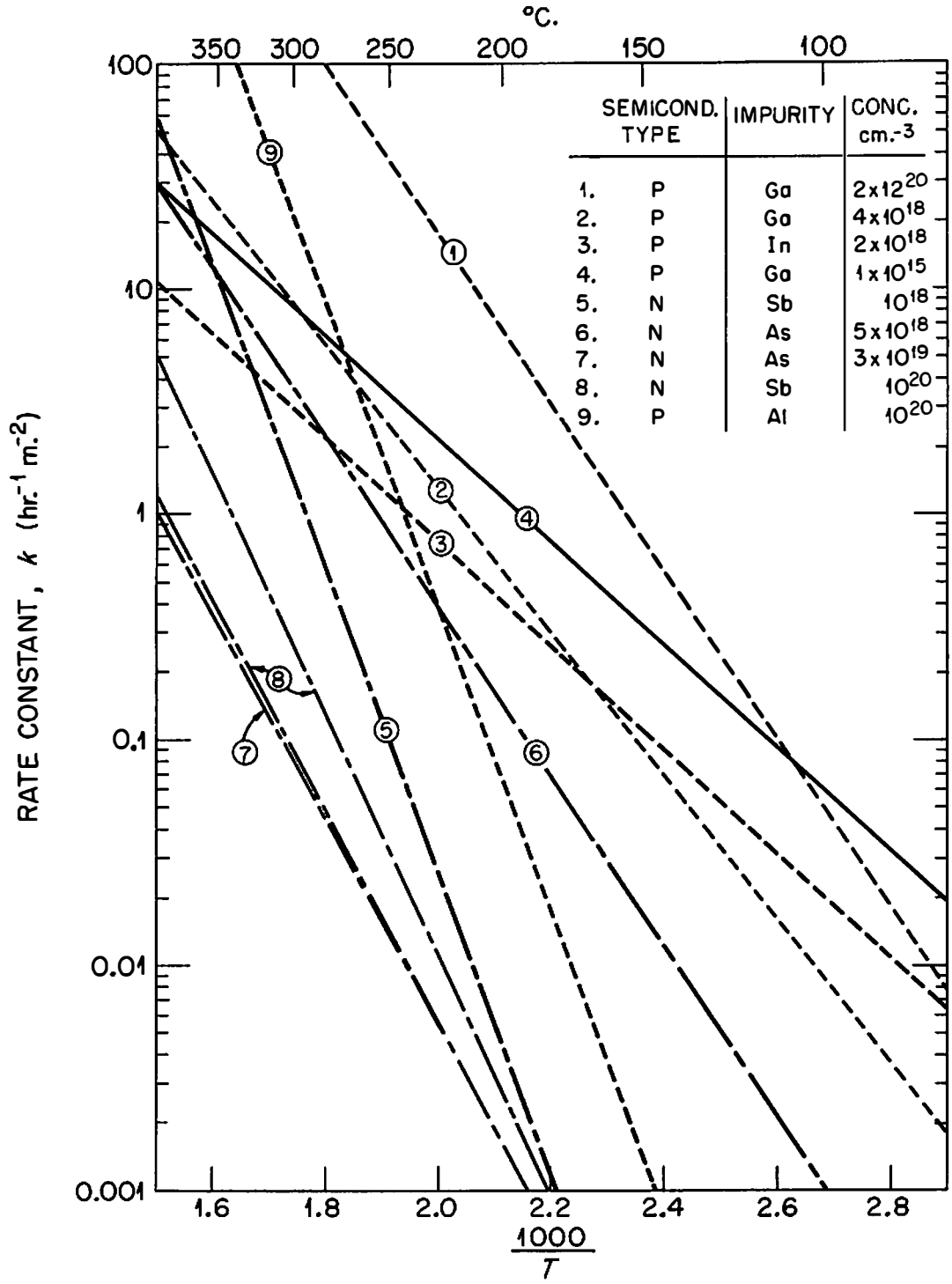

Figure 12. Arrhenius temperature dependence of first-order rate constants of hydrogen-deuterium exchange on chemically-doped germanium (least-squares analysis).

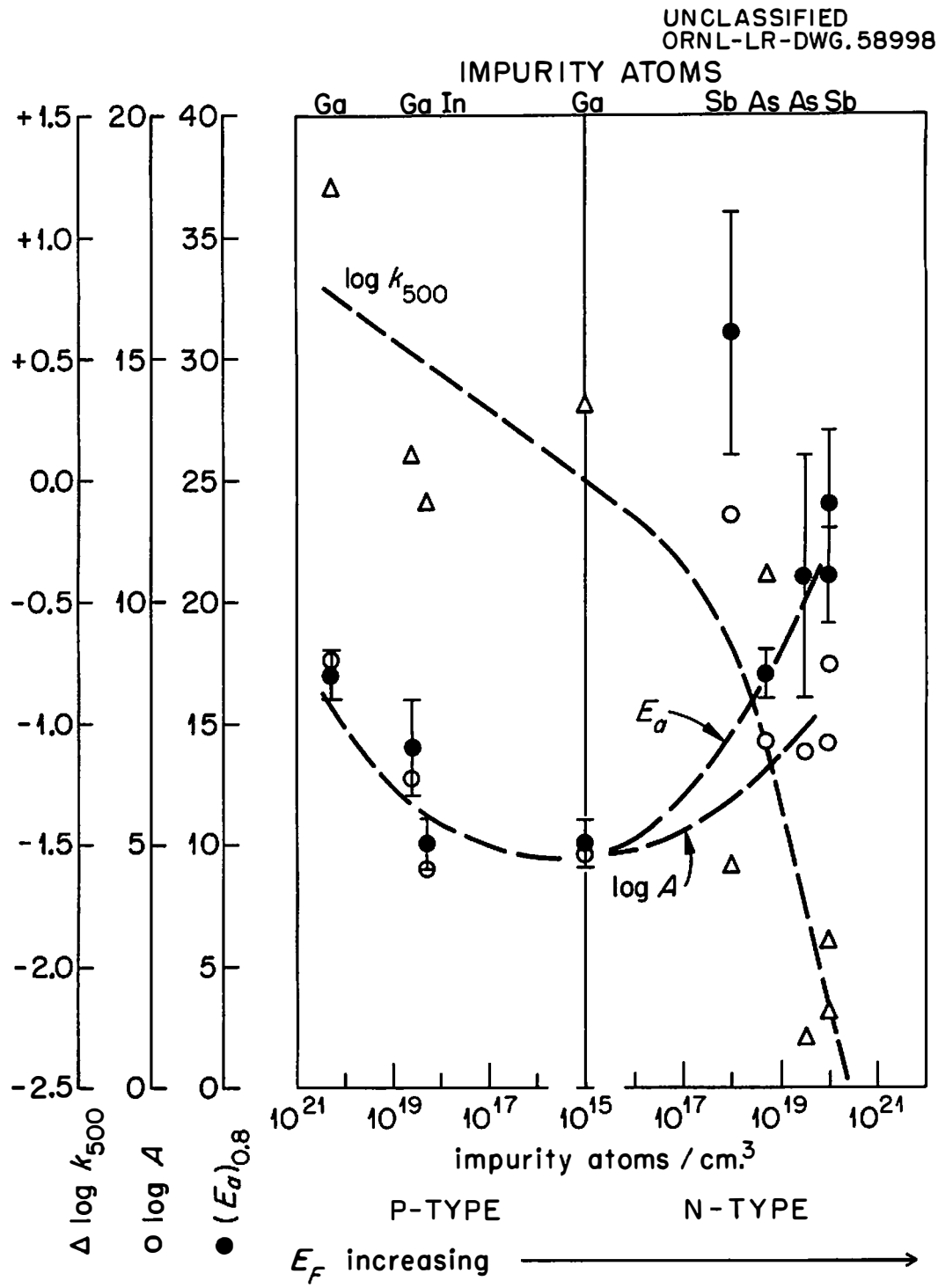

Figure 13. Correlation of kinetic factors of hydrogen-deuterium exchange with Fermi level of germanium.

0.013 e.v., they were essentially completely ionized at the temperatures of investigation. The concentrations of impurity atoms then also represent the concentrations of charge carriers, and the logarithm of this concentration is related to the Fermi level of the solid, as discussed in Chapter I. The abscissa of Figure 13, therefore, represents the Fermi energy (the electronic chemical potential).

Germanium doped with 1×10^{15} atoms gallium/cm.^{3}, operates as an intrinsic semiconductor above temperatures of about 130°.[65] Larger concentrations of particular impurity atoms position the Fermi level in the forbidden energy gap from near the edge of the valence band to the conduction band, as shown in Figure 5. The impurity atoms which were incorporated in the germanium used in this research appeared to provide charge carriers as expected, except for aluminum-doped samples which are discussed below; with this exception, there is no evidence of specific influence by any of the other impurity atoms.

The shape of the curve of activation energies for the exchange with respect to the electrochemical potential is an important feature of the results. A definite minimum in the activation energy occurs in the region near intrinsic semiconductivity, as can be seen by comparing the activation energies calculated at the 95 per cent confidence level:

Type	Impurities, cm.$^{-3}$	$(E_a)_{0.95}$
p	2×10^{20} Ga	17 ± 2
p	2×10^{18} In	10 ± 2
i	1×10^{15} Ga	10 ± 2
n	5×10^{18} As	17 ± 2
n	10^{20} Sb	21 ± 4

The energy of activation of the exchange, E_a, is related linearly to the logarithm of the frequency factor, log A, as shown in Figure 14. The result of this relationship is known as the "compensation effect" which is discussed later in this section.

In Figure 13 the activation energy of the exchange decreases as the semiconductivity of the solid is changed from highly n-type to intrinsic; the activation energy increases again on highly p-type germanium. Over this same range of semiconductivity, the rate constant at 500°K. (k_{500}) appears to increase. A large increase in rate occurs over the region from highly n-type to intrinsic semiconductivity; a much smaller increase (possibly even a constant rate) is seen to occur in the region toward highly p-type semiconductivity. Rates at 450° and 550°K. show trends with semiconductivity similar to those at 500°K.

2. Formic Acid Decomposition

The B_2O_3-dried formic acid was used in almost all the experiments. However, the fractionally-distilled formic acid was used in a few experiments to determine if different sources of the acid and different methods of drying had an effect on the decomposition rate. The two acids gave virtually identical results.

The rate of dehydrogenation of formic acid vapor on n-type germanium was so slow that it could not be detected relative to that occurring on the walls of the reaction vessel (Figure 10). It was estimated that k_{CO_2} at 500°K. must be less than about 10 micromoles $hr.^{-1}$ $m.^{-2}$ on n-type germanium. Since dehydrogenation is relatively rapid on p-type

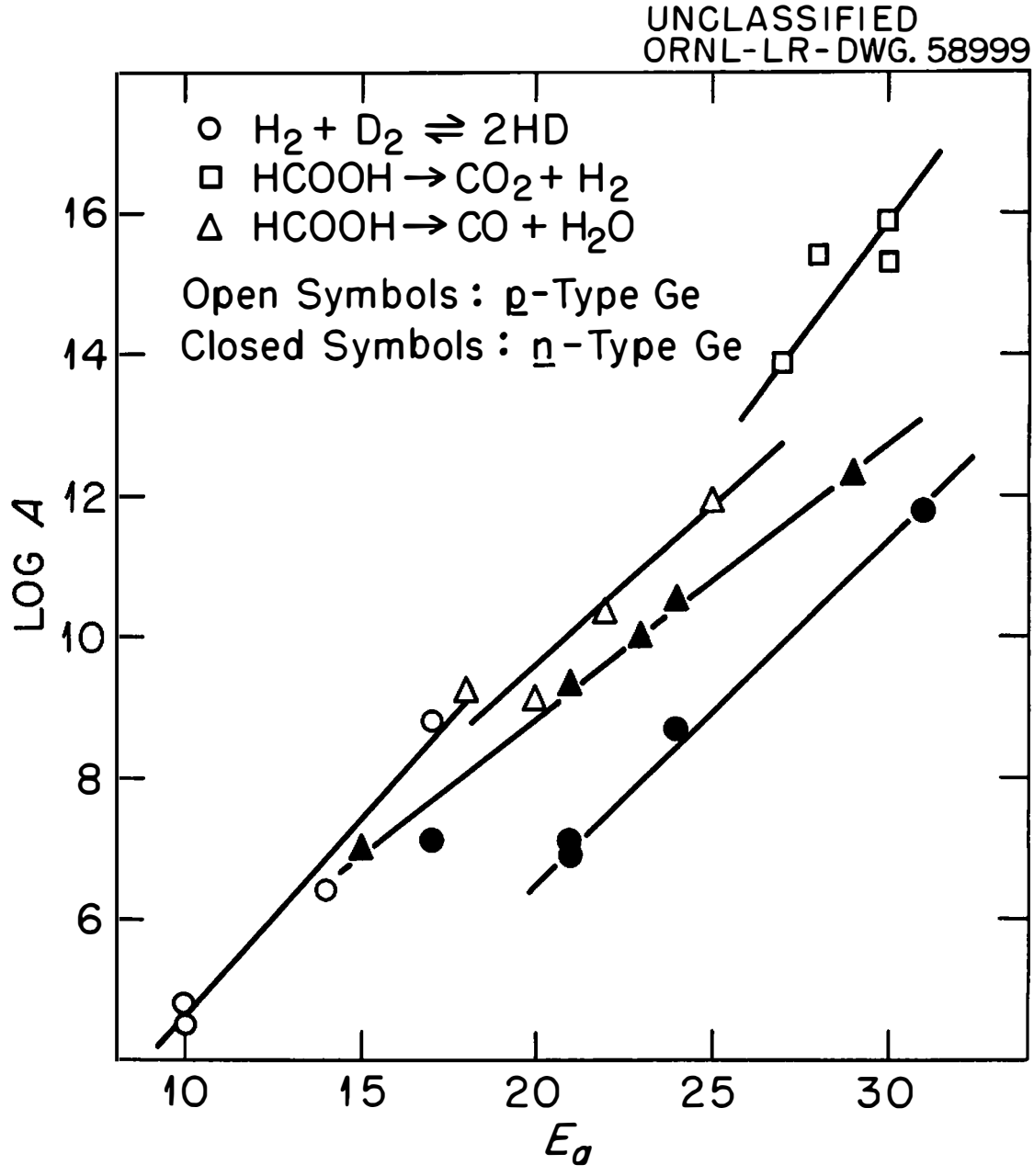

Figure 14. Relation between apparent activation energy and frequency factor for exchange and decomposition reactions on germanium.

germanium, it may be inferred that the activation energy for dehydrogenation is lower on p- than on n-type germanium. Assuming that the frequency factors are about the same for the reaction on both types of germanium, the differences in rates at 500°K. can be accounted for by a difference in activation energies of about 4 kcal./mole.

The results of the decomposition of formic acid are summarized in Table V. Dehydrogenation is considerably faster on p-type germanium than on n-type (approximately >20-400 times at 500°K.) while dehydration is only slightly faster (~5-25 times). For p-type germanium, dehydrogenation is the chief path of decomposition.

As with the exchange, a linear relationship exists between log A and E_a as seen in Figure 14.

A complication in the interpretation of the decomposition results would exist if the water gas equilibrium:

$$CO_2(g) + H_2(g) \rightleftharpoons CO(g) + H_2O(g) \qquad (26)$$

were operative under the experimental conditions. This possibility is discussed in the following section.

3. Water Gas Equilibrium

Although formic acid can decompose in several different ways to yield a variety of products, it seems quite certain that on germanium (and on other materials, as discussed previously) formic acid decomposes chiefly by dehydrogenation and, to a lesser extent, by dehydration. However, there is the possibility that the distribution of decomposition products may be affected by the water gas equilibrium. In the extreme, the decomposition

may be entirely by either of these processes, while the other group of products appears as a result of the water gas equilibrium, for example:

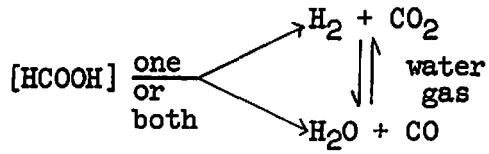

(27)

It appears, however, that the water gas equilibrium did not operate under at least most of the conditions of the experiments and, therefore, equilibration of reaction products need not enter into considerations of the decomposition mechanism. This conclusion was reached by comparing the observed ratio of CO/CO_2 with the theoretical value that was calculated from the equilibrium constant, K, for the water gas reaction. For the reaction written in Equation (26), the equilibrium constant is:

$$K = \frac{[CO][H_2O]}{[CO_2][H_2]} \tag{28}$$

The variation of K with temperature can be expressed by the equation:

$$\log K = 2.231 - \frac{2183}{T} + 0.110 \log T \tag{29}$$

which gives values of K in agreement with literature values.[88]

Under normal circumstances, dehydrogenation of formic acid will produce equal amounts of hydrogen and carbon dioxide, while dehydration will produce equal amounts of water and carbon monoxide. Since

$$[H_2] = [CO_2] \tag{30}$$

and

$$[H_2O] = [CO], \tag{31}$$

Equation (28) becomes:

$$K = \frac{[CO]^2}{[CO_2]^2} \tag{32}$$

Therefore, $K^{1/2}$ represents the ratio CO/CO_2 at equilibrium, under these conditions.

However, the concentrations of carbon dioxide and hydrogen were not equal in the gas phase over p-type germanium, as discussed previously; under these conditions, Equation (30) is not correct and the relationship shown in Equation (32) would not quite apply. However, the ratio of H_2/CO_2 in the gas phase may be considered constant:

$$\frac{[H_2]}{[CO_2]} = S \tag{33}$$

Substitution of this relationship into Equation (28), assuming that the expression in Equation (31) is still valid, yields:

$$K = \frac{[CO]^2}{S[CO_2]^2} \tag{34}$$

Therefore, for the situation in which the ratio H_2/CO_2 in the gas phase is not unity, but is constant:

$$\frac{[CO]}{[CO_2]} = (SK)^{1/2} \tag{35}$$

Since the ratio of H_2/CO_2 (i.e., S) was determined to be less than unity and probably near 0.4 in the gas over p-type germanium, the theoretical ratio of CO/CO_2 will be somewhat less than $K^{1/2}$, probably about 0.6 $K^{1/2}$, in these cases.

Figure 15 shows the ratios of CO/CO_2 which were determined in the gas phase following the decomposition on several of the catalysts, as a function of the temperature at which the decomposition took place. The results which were selected for illustration in Figure 15 are typical of the experimental data, and show that the observed ratios were generally

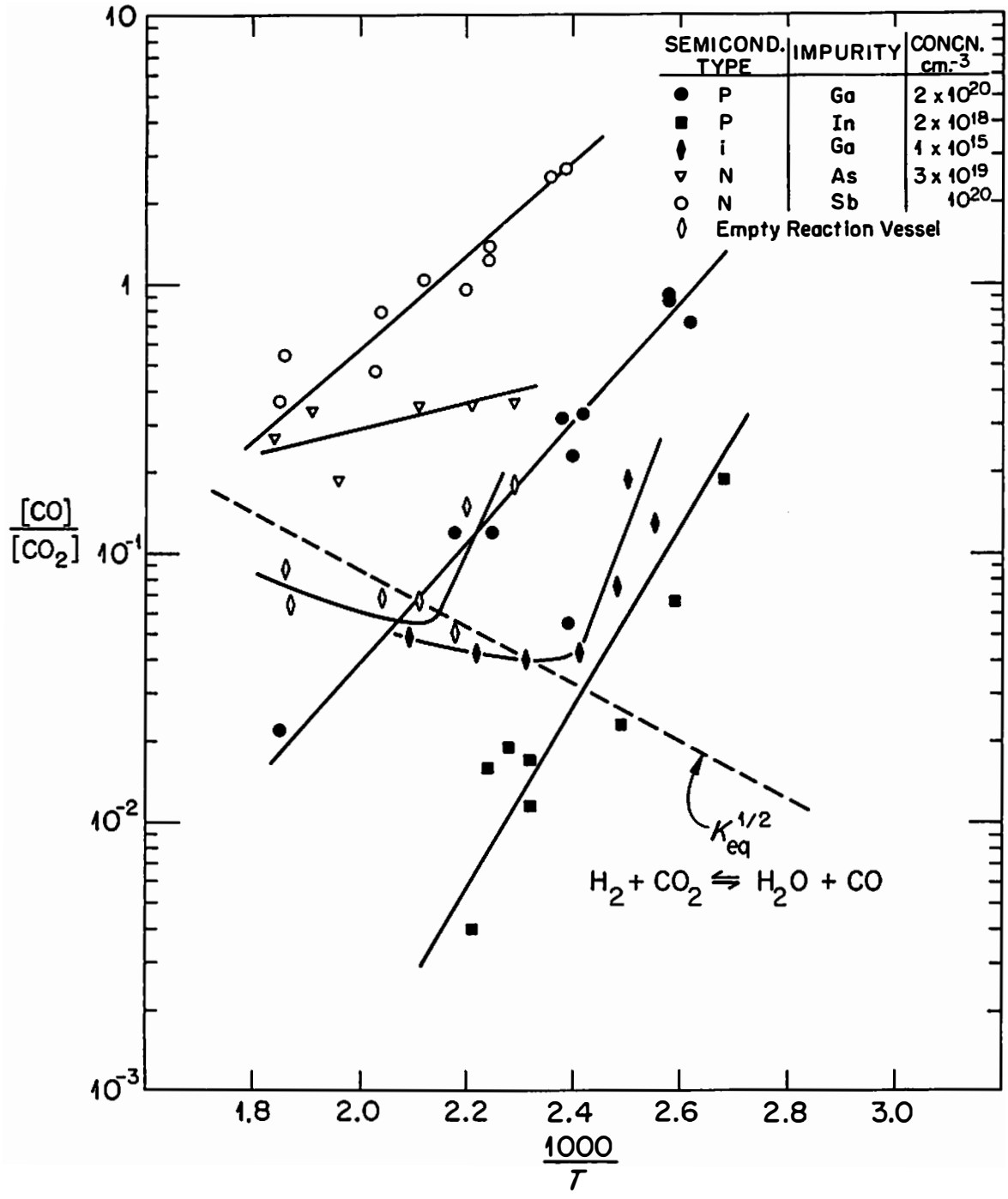

Figure 15. Temperature dependence of the ratio CO/CO_2 from decomposition of formic acid.

considerably different than the values computed from the equilibrium constant for the water gas reaction. Furthermore, the observed ratios varied oppositely with temperature than the theoretical ratios. These observations suggest that for the most part the water gas equilibrium did not significantly affect the distribution of products of the formic acid decomposition. Such products appear to be produced, therefore, in primary decomposition processes.

The decrease in the observed ratio CO/CO_2 with increasing temperature is interpreted as due to the larger temperature dependence (activation energy) of the dehydrogenation mechanism as compared to that for the dehydration process. Thus, increasing temperature should increase the rate of dehydrogenation more than the rate of dehydration, and cause the ratio CO/CO_2 to decrease.

With increasing temperature of decomposition, however, the ratio in some cases ceased to decrease and began to increase more or less parallel to the theoretical ratio calculated from the equilibrium constant for the water gas reaction. This result strongly suggests that the water gas equilibrium had begun to control the distribution of products in the decomposition. Such behavior occurred in the empty reaction vessel for temperatures above about 180° (Figure 15). However, the behavior was not observed in any of the reaction vessels containing n-type germanium, in spite of the fact that temperatures up to 270° were used. This observation suggests that when formic acid decomposes directly on quartz surfaces, the products are distributed according to the water gas equilibrium, but that quartz surfaces are not able to equilibrate products which result

from the decomposition on other surfaces. Thus it appears that formic acid poisons quartz as a catalyst for the water gas reaction; similar results for magnetite catalysts have been reported.[89]

However, the data (typically represented in Figure 15) suggest that in general the water gas equilibrium does not significantly influence the distribution of products of the decomposition of formic acid on germanium, and especially not at the lower temperatures of decomposition. Similar conclusions have been reached for other systems.[80, 90, 91]

4. Aluminum-Doped Germanium

The kinetics of the hydrogen-deuterium exchange on surfaces of n- and p-type germanium are clearly dissimilar, the rate generally being faster and the apparent activation energy somewhat lower on the latter (Figure 12). However, the exchange on aluminum-doped germanium showed behavior unlike that on other Group III-doped samples (Figure 12 and Table V). Because this anomalous behavior was reproducible, it appeared to be a real property of the solid.

This effect with aluminum-doped germanium may be related to a phenomenon that has been shown to occur with aluminum in silicon;[92] of all Group III acceptor solutes, only aluminum reacts sufficiently with dissolved oxygen to be transformed nearly completely into a donor complex. Since the reaction mechanisms and donor structures in the equilibria for the system germanium-oxygen are so similar to those for silicon-oxygen,[93] it seems likely that aluminum impurities might react with oxygen similarly in both host crystals. Therefore, aluminum-doped germanium is believed

to be atypical of Group III dopings and, although the results using this material are reported (Table V), they are not included in the analysis of the catalytic data on germanium.

Anomalous results with aluminum antimonide in the decomposition of ethanol were suggested by Schwab[56] to be due to aluminum oxide in the surface layers.

5. Compensation Effect

It has frequently been observed that values of rate constants do not vary as much as would be expected from changes in activation energy. Studies of the relationships between factors in the Arrhenius equation:

$$k = Ae^{-E_a/RT} \qquad (23)$$

led to recognition of the compensation effect; that is, a linear relationship between the activation energy (E_a) and the logarithm of the frequency factor (A). This correlation was shown in the present studies on germanium in Figure 14.

Tuul and Farnsworth[94] have very recently reported a compensation effect in their work and have given a brief summary of the pertinent literature. Quite a few theoretical explanations of the phenomenon have been advanced, some of which are discussed by Tuul and Farnsworth or in the references cited by them.

Another explanation of the effect has been advanced by Weisz[95] based on his model of chemisorption on semiconductors. He considers the individual rates of adsorption, desorption, and conversion of all species in deriving the kinetics of the catalytic reaction. The rates of chemisorption are believed to be limited by the rate of transfer of electrons

between the solid and chemisorbate, and are shown to have the form $Ae^{-qV/kT}$, where V is the potential barrier set up in the boundary layer of the semiconductor due to electron transfer (Figure 6). Since V is a function of the total number of atoms chemisorbed, an interdependence of "frequency factors" and "activation energies" is suggested, increasing activation energy accompanying increases in frequency factor.

CHAPTER IV

DISCUSSION

Almost all the experimental results relating semiconductivity and heterogeneous catalysis have been obtained with metallic oxides. Such oxides have not been entirely satisfactory solids to use for such correlations, because they are often complex materials which are by no means thoroughly understood. It is known, for example, that the catalytic activity of many oxides is very sensitive to their pretreatment conditions; at elevated temperatures oxygen may be lost from the surface, or surface ions may be affected by gaseous atmospheres. Perhaps the most serious limitation to oxides as semiconducting solids is that although their electronic structure may be modified through incorporation of small amounts of altervalent ions, the type of semiconductivity remains either n- or p-type and only the degree of this character can be changed. Thus, a thorough investigation of the influence of semiconductivity on a catalytic reaction requires that two different oxides be used as catalysts: an oxide of n-type character (e.g., zinc oxide) and an oxide of p-type character (e.g., nickel oxide). Furthermore, samples of oxides which possess different concentrations of charge carriers are prepared by incorporating different impurity atoms at varying concentrations into the host crystal; the physical properties of such samples are apt not to be the same, for the sintering properties of oxides containing even small amounts of impurities often differ widely, and could result in widely different surface properties.

Such remarks must not be taken as criticizing the use of defect oxides as semiconductors in catalytic studies. Without doubt such investigations have been of great significance in the field of catalysis. Awareness of the limitations of defect oxides as catalysts in such studies is essential, however, so that the results may be evaluated in the proper perspective.

Chemically-doped elemental germanium seems considerably more attractive than defect metallic oxides as semiconducting catalytic solids, especially under reducing conditions. However, little work using germanium (or other metalloids, or intermetallic compounds) has been possible until recently because neither high-purity germanium nor germanium of controlled impurity content has been available. Extrinsic germanium, as a catalyst, is not subject to the limitations described above for metallic oxides, and an investigation of catalytic reactions on chemically-doped germanium should add to the knowledge of the relationship between catalysis and semiconductivity.

The research, which is described in this thesis, used chemically-doped, elemental germanium as the catalytic solid to obtain experimental data which, it is hoped, may be helpful in extending concepts relating catalysis and semiconductivity. The results will be interpreted along lines developed with oxide catalysts; they will be seen to agree quite well with previous results in some cases (formic acid decomposition), but to disagree in certain others (hydrogen-deuterium exchange on zinc oxide). The disagreement is considered due to incomplete knowledge about the surface properties of oxides, rather than a serious difficulty in theory.

The previous chapter included several interesting corollaries of the catalytic study: the possible influence of the water gas equilibrium in the decomposition of formic acid, and the presence of nonstoichiometric concentrations of products in the gas phase upon dehydrogenation of formic acid on p-type germanium. In this chapter it will be attempted first to discuss mechanistic interpretations of the catalytic results on chemically-doped germanium, and, second, to compare these results with related work in the literature.

A. Proposed Mechanisms

In order to discuss reaction mechanisms, some form of expression is required to convey ideas. In the present discussion, a symbolism based on convenience of presentation is used, but the limitations of the representation must first be outlined.

First of all, electron transfers between solid and adsorbate have been thoroughly considered. Dowden[26] described heterogeneous catalysis on the basis of electron exchanges between catalysts and adsorbates. Boudart[95] outlined a relationship between adsorption and the Fermi level in semiconductors, while Weisz,[96, 97] Aigrain and Dugas,[98] and Hauffe and Engell[99] have independently considered effects of electronic charge transfer between adsorbate and solid and have treated chemisorption on semiconductors as an electronic boundary layer problem. In the work described in this thesis, kinetic factors for the hydrogen-deuterium exchange and formic acid decomposition on chemically-doped germanium have been

shown to be related to the semiconductivity of the solid (Figure 13 and Table V), and electronic processes between semiconductor and adsorbate appear to operate. It is convenient to think of these processes as electron transfers between gaseous adsorbate and solid adsorbent. However, it may be better to speak of "electron shifts," since the experiments contribute no information to the nature of these electronic processes other than to suggest that they are rate controlling. The electronic bonding between adsorbate and solid is unknown; it may vary from purely homopolar to ionic or be any degree in between. However, it becomes convenient to represent chemical and electronic action on the surface of the solid by an ionic formalism, after Hauffe,[29] and to speak of electron shifts or transfers even though polarization or bonding of varying ionic character may describe the actual interactions more accurately.

In the processes to be described later in this chapter, a formula in brackets will be used to represent a surface species of purely speculative arrangement. A plus sign indicates that there has been a shift of electrons away from the species, and a minus sign indicates that there has been a shift of electrons towards the species. Such a species may exist in a polarized or covalently-bound or partially or completely ionized state on the surface. The symbol $\ominus$ refers to quasi-free electrons in the solid, and $\oplus$ refers to mobile holes.

Since the rate-determining steps in the exchange and dehydrogenation reactions on germanium appear to be processes involving shifts of electrons between adsorbate and solid, the electronic properties of the semiconductor, i.e., its electronic chemical potential (Fermi level), are expected to

determine in part the direction and energetics of such electron motion. The experiments, therefore, have been interpreted in terms of the Fermi level of the semiconductor.

1. Hydrogen-Deuterium Exchange

Figure 13 summarizes the variations in kinetic parameters of the heterogeneous exchange with the Fermi level of the catalyst. Such variations strongly suggest that the electronic character of the solid influences the kinetics of the reaction occurring on its surface. In fact, the minimum in the activation energy curve with respect to the electronic chemical potential of the solid suggests that two different electron-controlled rate processes are operating, since a monotonic change in kinetic factors with Fermi level would be expected for a single rate-limiting step.

One rate-determining reaction mechanism may be the shift of electrons from adsorbate to solid. In the context of the ionic formalism suggested above, this step may be represented:

$$H_2 \rightarrow 2[H^+] + 2\ominus \qquad (36a)$$

As emphasized above, this representation is purely symbolic; it has been hoped to avoid the implication that the process expressed in Equation (36a) is definitely believed to occur. Other equations may be written to express the idea that there is a shift of electrons from the adsorbate to the solid:

$$H_2 + D_2 \rightarrow 2[HD^+] + 2\ominus \qquad (36b)$$

or

$$H_2 \rightarrow [H_2^+] + \ominus \qquad (36c)$$

A second rate-determining process may be the shift of electrons in the opposite direction, i.e., from solid to adsorbate:

$$[H^+] + [D^+] \rightarrow HD + 2 \oplus \qquad (37a)$$

or

$$[HD^+] \rightarrow HD + \oplus \qquad (37b)$$

or

$$[H_2^+] + [D_2^+] \rightarrow 2HD + 2 \oplus \qquad (37c)$$

In the region of n-type semiconductivity of Figure 13, the apparent activation energy of the exchange decreases and the velocity increases as the electronic chemical potential of the solid decreases. These results seem most easily explained by a rate-controlling process requiring an electron shift from adsorbate to solid, since the potential barrier to such a process would be expected to diminish as the free-electron concentration of the solid is decreased. This process may be a chemisorptive step, such as shown in Equations (36).

That chemisorption is the slow rate-controlling step in the region of n-type semiconductivity seems reasonable when one considers that quasi-free electron charge carriers predominate and might be expected to facilitate processes involving electron shift from solid to adsorbate, such as Equations (37), but to limit processes such as represented by Equations (36).

With continuing decrease in Fermi level the chemisorptive process appears to become so favored that it no longer is the slow step, and another process then determines the rate of the exchange. This transition in rate-determining processes appears to occur approximately in the region

of intrinsic semiconductivity; the activation energy of the exchange begins to increase as the Fermi level continues to decrease. This circumstance would be expected if the rate-controlling step were an electron shift from solid to adsorbate, a process such as that represented by Equations (37). The barrier to such a process would be expected to increase as the electronic chemical potential of the solid decreased.

Furthermore, p-type semiconductivity is characterized by an excess of (mobile) hole charge carriers. In this regard, Equations (37) may be seen to be limited by the concentration of free holes, and Equations (36) to be facilitated by their presence.

It is to be remembered that the experimental results suggest only that electron shifts occur between solid and substrate, and that these control the rate of the isotopic exchange. The symbolic equations, expressed above as Equations (36) and (37), are useful in describing these events. In more general terms, a molecule of hydrogen can be considered as it approaches the surface of the semiconductor. The molecule reacts (possibly becomes covalently linked) with an acceptor center on the surface; a partial, but not complete, electron transfer from the adsorbate to the acceptor center occurs and the process weakens the bond between the hydrogen atoms. Complete dissociation can, but does not necessarily have to, occur. These entities on the surface may now be in a position to interact; they may then react with donor centers in the surface, electrons being transferred from donor center to adsorbate, followed by desorption. Electron transfer, or shift, between adsorbate and adsorbent, in one direction or the other, may be the rate-limiting process, and electrons may

have to cross the potential barrier in the surface of the semiconductor. Thus, the activation energy for the chemical reaction catalyzed on the surface of the solid may arise in the electrostatic potential barrier in the surface of the semiconductor.

In the exchange reaction, product hydrogen deuteride may be formed by many reactions other than those symbolized in Equations (36) and (37), for example:

$$[H^+] + D_2 \rightarrow HD + [D^+] \tag{38a}$$

or

$$[D^+] + H_2 \rightarrow HD + [H^+] \tag{38b}$$

or

$$[H^+] + D_2 \rightarrow [HD^+] + D \tag{38c}$$

followed by

$$D + H_2 \rightarrow HD + H \tag{38d}$$

However, such steps do not involve a net electron interchange with the solid, and therefore, they cannot be the rate-controlling steps in the exchange. Furthermore, if they occur at all, they cannot be so rapid as to make the exchange appear independent of the electronic properties of the solid.

Speculations involving electron exchange between adsorbate and solid might consider $[H^-]$ as well as $[H^+]$. Of these, $[H^-]$ is thought a less attractive possibility than $[H^+]$; experimentally,[100] adsorption of oxygen on germanium increases the work function while adsorption of hydrogen decreases it, in support of the idea of $[O^-]$ and $[H^+]$ in the formalism used here. Therefore, rate-determining reactions seem more

reasonably represented by Equations (36) and (37) than by processes involving [H^-].

Previous investigators have sought to determine the relationship between hydrogen-deuterium exchange and semiconductivity of solids using defect oxides. In almost all such studies, pretreatment of the solid with hydrogen at high temperature (>350°) was found necessary for catalytic exchange to occur. It has been suggested that the reaction was between hydrogen or deuterium and surface OD or OH groups,[101, 102] or associated with partial surface reduction.[103] A very careful study of the exchange on defect zinc oxide (an n-type semiconductor) was reported by Molinari and Parravano,[102] whose results are directly opposite to those on n-type germanium reported here. Parravano and Boudart[104] consider the exchange mechanism on zinc oxide to be obscure because of several complicating factors. Equations (36a) and (37a) are similar to those proposed by Hauffe[29] to explain the exchange; he proposed Equation (37a) as the rate-determining step to explain Molinari and Parravano's results, whereas Equations (36) seem to be the likely slow rate-determining step on n-type germanium.

A minimum in the curve of activation energy of the decomposition of nitrous oxide versus semiconductivity (impurity concentration in nickel oxide) has been interpreted by Hauffe[29] to be the result of two rate-determining processes.

2. Formic Acid Decomposition

In the hydrogen-deuterium exchange just considered, different reaction mechanisms were seen likely to control the rate of the exchange,

depending on the particular electronic character of the solid. The semiconductivity of the solid may in a similar fashion influence the competition between alternate paths of reaction. Thus, it seemed appropriate to consider the influence of two-carrier semiconducting germanium catalysts on the decomposition of formic acid.

Table V shows that dehydrogenation of formic acid was relatively rapid on p-type germanium, but that the rate was immeasurably slow on n-type germanium. This difference in activity can be accounted for by a 4 kcal./mole larger activation energy on n-type than on p-type germanium. No statistically significant difference in activation energies for dehydrogenation was observed between intrinsic and highly p-type germanium. These results are in qualitative agreement with Schwab[56] who found that apparent activation energies for dehydrogenation of formic acid were greater on n- than on p-type germanium, and that the degree of doping was without influence.

The results for the dehydrogenation of formic acid vapor on germanium may be most simply explained by considering that the rate-determining step is a process involving a shift of electrons from adsorbate to solid. This process becomes more favored as the Fermi level of the solid decreases. In terms of the ionic formalism used previously, the process may be represented:

$$2[HCOO^-] \rightarrow H_2(g) + 2CO_2(g) + 2 \ominus \qquad (39)$$

This directional shift of electrons has often been postulated for the decomposition of formic acid on metals,[25, 105, 106] and to explain the increase in activation energy with increasing electron concentration

of alloys.[25, 105] On the other hand, Fahrenfort et al.[90] consider that the decomposition on all metals proceeds via a formate intermediate, and that the adsorbate attracts electrons from the metal and becomes negatively charged. Although such results are said not to support the electronic factor concept, the authors do not reject the possibility of a relationship between catalytic activity and electronic structure of the metal; in this instance they prefer to correlate the catalytic activities of individual metals with the bond energies of the metal formates. However, in a sense an "electronic factor" is involved even here.

Many studies of the catalytic decomposition of formic acid on metals, and of the adsorbed state of the acid by means of the infrared technique have been reported recently. However, the mechanism of the decomposition and the nature of adsorbed reaction intermediates are not well understood.[107, 108, 109]

The activation energy of the dehydration of formic acid on germanium varied randomly with chemical doping, and, to a first approximation, appeared independent of the electronic chemical potential of the solid. This suggests that the decomposition probably did not involve electron interchange between adsorbate and solid in the rate-controlling step. Dehydration of formic acid possibly takes place in a physically adsorbed layer.

B. Relevant Literature

1. Hydrogen-Deuterium Exchange

The exchange on germanium has been studied by Boreskov and Kuchaev[46] in the temperature range between 300° and 550° using (intrinsic) single

crystals which were treated with a hydrogen-deuterium mixture at 630°, and then crushed to a specific surface area of 55 to 71 cm.^{2}/g. The activation energy for the exchange was 17 kcal./mole and the specific rate constant at 300° was 3 x 10^{-10} moles cm.$^{-2}$ sec.$^{-1}$. In the work of this thesis, the apparent activation energy on intrinsic germanium in the temperature range 25° to 360° was 10 ± 1 kcal./mole with higher values being measured on the chemically-doped material; at 300° the rate constant was approximately 10 hr.$^{-1}$ m.$^{-2}$ or about 4 x 10^{-12} moles cm.$^{-2}$ sec.$^{-1}$.

There was probably sufficient difference in the preparation of the catalysts in these two investigations to account for these differences in activation energy and in catalytic activity. For example, the germanium catalysts of Boreskov and Kuchaev were prepared by crushing single crystals after high-temperature treatment; these samples must have been rather coarse, based on the reported surface areas, and surface defects probably were created during the crushing process. In the work of this thesis, the germanium catalysts were first mechanically ground, and were then treated with hydrogen at high temperature which probably annealed out much of the surface damage caused by grinding.

Sandler and Gazith[47] found an activation energy of 1.6 kcal./mole for the exchange reaction on sputtered germanium films in the temperature range 77° to 180°K. The remarkably high exchange activity was concluded to be due to a highly disordered structure. However, Farnsworth *et al.*[110] were unable to detect exchange on germanium at 170°, even after argon ion bombardment which extensively disrupts the surface; the technique was sufficiently sensitive to have readily observed the exchange on clean

surfaces, and, based on Sandler's data, even to have detected it on oxidized surfaces. The possibility of contamination in Farnsworth's system seems remote.

The mechanism of the hydrogen-deuterium exchange on metals does not appear to be a single, universal process, the same on all metals under all conditions, but rather seems best described by several processes, one or another predominating in any specific case. At least two mechanisms have been proposed, and are generally considered; both start with the dissociative chemisorption of hydrogen on the surface of the metal (represented M):

$$H_2 + 2\,M \rightarrow 2\,M\text{-}H \qquad (40)$$

In the Rideal-Eley mechanism, reaction involves a chemisorbed atom and a molecule from the gas phase or from the van der Waals layer, for example:

$$M\text{-}H + D_2 \rightleftharpoons M\text{-}D + HD \qquad (41)$$

The Bonhoeffer-Farkas mechanism involves reaction in the chemisorbed layer by combination of atoms; first, a process similar to Equation (40):

$$D_2 + 2\,M \rightleftharpoons 2\,M\text{-}D \qquad (42)$$

and then

$$M\text{-}D + M\text{-}H \rightleftharpoons 2\,M + HD \qquad (43)$$

A third mechanism, known as the Langmuir-Hinshelwood, has been discussed recently by Schwab;[111] it involves exchange between adsorbed molecules:

$$M\text{-}H_2 + M\text{-}D_2 \rightleftharpoons 2\,M\text{-}HD \qquad (44)$$

The similarity between these mechanisms, which have been proposed for the exchange on metals, and those suggested earlier as possibilities for the exchange on a semiconducting solid (i.e., germanium) is obvious,

for example: Equations (40) and (36a), Equations (41) and (38a), Equations (43) and (37a), and Equations (44) and 37c).

The mechanism, which predominates during the exchange on metals, often cannot be clearly established. With germanium it seemed possible to describe rate-determining steps in terms of electron shifts between solid and adsorbate, but impossible to define the precise steps involved in the process.

The general requirement for metals to chemisorb hydrogen readily and to possess hydrogenating catalytic activity now seems related to the presence of low-lying, unfilled (but not too empty) d-band orbitals. Such metals are able to accept electrons from hydrogen and to form weak bonds with it. As an element with loosely held valence electrons is added in solid solution, a decrease in catalytic activity is often observed; this decrease parallels the decline in the number of holes per atom in the d-band of the alloy, and suggests that electron shifts from adsorbate to metal are rate controlling.[26] However, only in very simple cases can the band theory be used to describe in detail the catalytic characteristics at the Fermi surface of alloys, because many other factors are often involved (e.g., interstitial hydrogen).

The hydrogen-deuterium exchange on many oxides has been reported,[112,113] but the fundamental significance of such results is not entirely clear because the properties of the oxides are by no means thoroughly understood.

Defect zinc oxide was the catalyst employed by Molinari and Parravano[102] in their very careful investigation of the effect of semiconductivity on catalysis, using the hydrogen-deuterium exchange as the

test reaction. Their results for the dependence of the activation energy and of the rate of exchange on the concentration of free electrons in the zinc oxide are exactly opposite those reported in this thesis for n-type germanium. This disagreement requires consideration.

Parravano and Boudart[104] have discussed the results on defect zinc oxide and their limitations, which are numerous. A number of complicating effects (such as nonlinear Arrhenius plots and a great sensitivity of the rate data to the mode of pretreatment of the oxide) obscure the exchange mechanism. It was suggested[102] that the exchange was between hydrogen or deuterium and hydrogenated surface compounds (surface OD or OH groups). It seems unlikely that an unambiguous explanation of the exchange results is possible because of the complex nature of the surface properties of the zinc oxide. These complexities probably also account for the apparent disagreement in results with germanium.

An interesting aspect of the exchange on zinc oxide has been provided by Harrison and McDowell,[114] who found results which also imply a dependence of catalytic activity on electron concentration of the solid just opposite to that found by Molinari and Parravano. Although zinc oxide or α,α-diphenyl-β-picrylhydrazyl (DPPH, a solid free radical) separately showed very little hydrogen-deuterium exchange activity at 77°K., a mixture of the two gave rapid and reproducible exchange. It was suggested that the catalytic activity of zinc oxide was enhanced by electron transfer to the DPPH, implying that a smaller concentration of free electrons in zinc oxide brought about increased catalytic activity. This conclusion is directly opposite that of Molinari and Parravano, but is in agreement with the results of this thesis. This interpretation is

supported by experiments[115] in which the electrical resistance of films of aluminum or palladium was raised after films of DPPH were deposited on the metal; this suggests that electrons had been transferred from the conduction band of the metal to the DPPH and is in the same direction as postulated with zinc oxide.

2. Formic Acid Decomposition

The dehydrogenation of formic acid on chemically-doped germanium has been discussed by Schwab,[56] but dehydration was not reported. The dehydrogenation results were compared with those of this thesis in the previous section. Some of the published results on metals have also been discussed with regard to the electron transfer process postulated for the dehydrogenation on germanium.

Using III-V intermetallic compounds, as well as germanium, Schwab[56] found that the activation energies for hydrogenation (of ethylene) and dehydrogenation (of formic acid and ethanol) were greater on n-type than p-type semiconductors. Anomalous results were obtained in the decomposition of alcohol on aluminum antimonide, and were attributed to the presence of aluminum oxide in the surface layer. In this connection the anomalous behavior of aluminum-doped germanium should be recalled (Chapter III).

The decomposition of formic acid has been studied on refractory oxides,[80, 116] but attempts to study the decomposition on several semiconducting oxides have been complicated by reduction of the solid.[117] However, interesting results have been obtained by studying the decomposition of formic acid on metals supported on semiconducting oxides. Schwab[118, 119]

used nickel, cobalt and silver films vaporized unto aluminum oxide previously doped with appropriate impurity atoms to vary its n-type semiconductivity. Szabo used metallic nickel on several semiconducting oxides of both n- and p-type semiconductivity.[120, 121] Charge exchange at the metal-semiconductor contact was believed to influence the transition of electrons from substrate to metallic catalyst. Thus, as the Fermi level of the semiconducting oxide support decreased, the Fermi level of the metal with which it was in contact decreased, and the activation energy of the decomposition decreased.

Thus, the decomposition of formic acid on intermetallic compounds, on germanium, and on metal-metal oxide catalysts is similar: as the Fermi level of the solid decreases, the activation energy of the decomposition decreases.

CHAPTER V

SUMMARY

Rates and activation energies for the hydrogen-deuterium exchange and formic acid vapor decomposition were measured on a series of chemically-doped germanium catalysts over the temperature range 100° to 400°. The germanium catalysts were intrinsic, and n- or p-type extrinsic semiconductors; the position of the Fermi level of the solid was located suitably in the forbidden energy gap.

Kinetic parameters of the exchange and decomposition reactions were related to the Fermi level (electronic chemical potential) of the solid. Their dependence suggested that the rate-limiting processes involved electronic charge shifts between adsorbate and semiconductor.

Two different rate processes appeared to limit the hydrogen-deuterium exchange. A process involving an electron shift from adsorbate to solid appeared to control the rate in the region of n-type semiconductivity. In the region of p-type semiconductivity, the rate-determining process appeared to be an electron shift in the opposite direction (from solid to adsorbate).

Dehydrogenation and dehydration of formic acid on germanium were observed. Dehydrogenation was the predominant method of decomposition on p-type germanium; however, dehydrogenation on n-type germanium could not be detected. A process involving an electron shift from adsorbate to solid appeared to control the dehydrogenation reaction.

Dehydration of formic acid occurred on all germanium catalysts, and appeared independent of the Fermi level of the solid.

Both dehydrogenation and dehydration of formic acid appeared to be primary decomposition processes at the lower temperatures. There was evidence, however, that the water gas equilibrium affected the distribution of products at some of the higher temperatures that were used.

Nonstoichiometry of dehydrogenation products in the gas phase over p-type germanium was detected, and seemed to be best explained by the removal of hydrogen atoms by the germanium during the process of formic acid decomposition.

APPENDIXES

APPENDIX I

CALCULATION OF FIRST-ORDER RATE CONSTANTS FOR HYDROGEN-DEUTERIUM EXCHANGE

It is convenient to refer to α, the fraction of hydrogen deuteride formed in time t, and defined:

$$\alpha = \frac{x - x_o}{x_e - x_o} \tag{45}$$

where x refers to the fraction of hydrogen deuteride at time t; x_o, the fraction of hydrogen deuteride at time zero; and x_e, the fraction of hydrogen deuteride at equilibrium.

First-order rate constants can be calculated from the equation:[122]

$$k = \frac{1}{t} \ln \frac{x_e - x_o}{x_e - x} \tag{46}$$

Since

$$(1-\alpha) = 1 - \left[\frac{x - x_o}{x_e - x_o}\right] = \frac{x_e - x}{x_e - x_o} \tag{47}$$

and

$$\frac{1}{1 - \alpha} = \frac{x_e - x_o}{x_e - x} \tag{48}$$

Equation (46) becomes:

$$k = \frac{1}{t} \ln \frac{1}{1 - \alpha} \tag{49}$$

In terms of half-times for reaction, $t_{1/2}$;

$$t_{1/2} = \frac{\ln 2}{k} \tag{50}$$

and

$$t_{1/2} = \frac{0.301\ t}{\log \frac{1}{1-\alpha}} \tag{51}$$

Therefore, in order to calculate the first-order rate constant using Equation (49), or Equations (50) and (51), α must be evaluated, for which the values x, x_o, and x_e must be known. These values can be determined from mass spectrometric analyses.

x. The fraction of hydrogen deuteride at time t can be obtained directly by mass analysis of the gas which is sampled from the reaction vessel after t hours at some constant temperature. If the relative abundances of masses 2, 3 and 4 are A_2, A_3 and A_4, respectively, then:

$$x = \frac{A_3}{A_2 + A_3 + A_4} \tag{52}$$

x_o. The fraction of hydrogen deuteride at time zero can be obtained by the mass analysis of the unreacted exchange mixture, in the manner just indicated. The value of x_o was found experimentally to be approximately 3.0 ± 0.4 per cent hydrogen deuteride.

x_e. The fraction of hydrogen deuteride at equilibrium can be calculated from the equilibrium constant for the exchange:

$$H_2 + D_2 \rightleftharpoons 2\ HD$$

$$K = \frac{[HD]_e^2}{[H_2]_e[D_2]_e} \tag{53}$$

The equilibrium constant at the temperature of the exchange can be calculated from the equation:

$$K = 4.24e^{-79/T} \tag{54a}$$

or its equivalent:

$$\log K = -\frac{34.32}{T} + 0.6267 \tag{54b}$$

in agreement with results in the literature.[123, 124]

Using fractions, as in Equation (52), for the concentrations in Equation (53), and recalling that subscript e represents equilibrium values:

$$[HD]_e = x_e \tag{55}$$

and

$$[H_2]_e + [D_2]_e + [HD]_e = 1 \tag{56}$$

Experimentally, nearly 1:1 mixtures of hydrogen and deuterium were used. Therefore:

$$[H_2]_e \simeq [D_2]_e \tag{57}$$

In the three Equations (53), (56), and (57), there are only three unknowns, so that x_e, identical to $[HD]_e$, can be evaluated.

In general, exact values for x_e can be calculated and the approximation in Equation (57) is not required. The ratio of D/H for any sample may be determined from the relative abundances of masses 2, 3 and 4; this ratio is the same at equilibrium as at time t. Therefore, using the symbols from Equation (53):

$$\frac{D}{H} = \frac{A_4 + A_3/2}{A_2 + A_3/2} = \frac{[D_2]_e + x_e/2}{[H_2]_e + x_e/2} \tag{58}$$

Equations (53), (55), (56), and (58) now permit the calculation of x_e exactly.

In practice, however, values of x_e were calculated for several values of the ratio D/H near unity at several temperatures within the range of interest. A family of curves for x_e versus D/H at the several temperatures was drawn, so that x_e under the exact experimental conditions could be obtained readily. The ratio D/H was found to be

1.03 ± 0.08 for all the experiments. Consequently, the approximation given in Equation (57), and the resulting simplification in calculations, was valid.

APPENDIX II

CALCULATION OF RATE CONSTANTS FOR FORMIC ACID VAPOR DECOMPOSITION

In order to evaluate a consistent rate constant for the decomposition of formic acid vapor on germanium, the experimental data were corrected for the following:

(a) dimerization of formic acid vapor

(b) nonstoichiometry of dehydrogenation products in the vapor phase

(c) decomposition on quartz

(d) deviation from zero-order kinetics

These corrections will be discussed in order.

Formic acid vapor is associated; the vapor contains molecules both of dimer, $(HCOOH)_2$, and monomer. It is expedient to consider the formic acid in the completely dissociated state, i.e., monomeric. This is conveniently done by using the data of Coolidge[125] and others[126, 127] to construct a family of curves giving the fraction of dimer present at specific temperatures for pressures of formic acid.

As discussed in Chapter III, the decomposition of formic acid on germanium occurs predominantly by the following reactions:

$$HCOOH \rightarrow CO_2 + H_2 \qquad (18)$$

$$HCOOH \rightarrow CO + H_2O \qquad (19)$$

The gaseous sample, which was removed from the reaction vessel, was composed of decomposition products and undecomposed reactant (formic acid). A McLeod gauge was used to determine both the total amount of gas present in the sample (c_{total}) and that which did not condense at -78° (c_{-78}).

Care was taken not to exceed the vapor pressure of formic acid (42 mm. at 25°) in measuring c_{total}.

$$c_{total} = c_f + c_{H_2} + c_{CO_2} + c_{H_2O} + c_{CO} \tag{59}$$

$$c_{-78} = c_{H_2} + c_{CO_2} + c_{CO} \tag{60}$$

where c represents the amount of gas in cc.-mm., and c_f is the amount of residual formic acid vapor, both dimer and monomer.

The chromatographic data were used to obtain the following ratios:

$$S = c_{H_2}/c_{CO_2} \quad \text{and} \quad R = c_{CO}/c_{CO_2} \tag{61}$$

Therefore,

$$c_{H_2} = Sc_{CO_2} \quad \text{and} \quad c_{CO} = Rc_{CO_2} \tag{62}$$

Substituting these in Equation (60):

$$c_{-78} = Sc_{CO_2} + c_{CO_2} + Rc_{CO_2}$$

and

$$c_{CO_2} = \frac{c_{-78}}{S+R+1} \tag{63}$$

Thus, from the amount of gas noncondensable at -78° and from the chromatographic analysis, the amount of hydrogen, carbon dioxide, and carbon monoxide in the sample can be determined. The amount of undecomposed reactant is also required and can be estimated from Equation (59). In this equation only c_f and c_{H_2O} remain unknown. Although these quantities were not determined independently, stoichiometric considerations indicate that $c_{H_2O} = c_{CO}$ and c_f can readily be calculated. It may be noted here that, in general, the amount of undecomposed formic acid is relatively large compared to the amount of water, because formic acid decomposes chiefly by dehydrogenation, and very little by dehydration. In the case

for which $c_f \gg c_{H_2O}$:

$$c_{total} - c_{-78} \sim c_f \tag{64}$$

This amount of residual formic acid, dimer and monomer, can be converted to the amount of monomer alone, c_{HCOOH}, as previously indicated. The sum ($c_{HCOOH} + c_{CO_2} + c_{CO}$) represents the amount of (monomer) formic acid that would have been present in the sample if no decomposition had taken place. Let f_{CO_2} represent the fraction of carbon dioxide in the sample, and defined:

$$f_{CO_2} = \frac{c_{CO_2}}{c_{HCOOH} + c_{CO_2} + c_{CO}} \tag{65}$$

And, similarly, let

$$f_{CO} = \frac{c_{CO}}{c_{HCOOH} + c_{CO_2} + c_{CO}} \tag{66}$$

These ratios apply not only to the aliquot taken from the whole gaseous mixture, but to the mixture itself. Since the amount of monomeric formic acid present originally in the reaction vessel (n_o) can be calculated from P-V-T data at loading, assuming the ideal gas law and correcting for dimerization, the amount of carbon dioxide (n_{CO_2}) or carbon monoxide (n_{CO}) produced in the reaction vessel is the product of n_o and f_{CO_2} or f_{CO}.

These amounts of carbon dioxide and carbon monoxide, when divided by the time of decomposition, yield zero-order rate constants for the dehydrogenation and dehydration reactions, respectively. The rate of the decomposition on quartz alone was determined from data for empty reaction vessels. Comparison of data for empty reaction vessels and for those

containing germanium, revealed that no significant dehydrogenation occurred on n-type germanium; the decomposition that was found apparently arose entirely from decomposition on quartz (Figure 10). Corrections to the observed rates on germanium for that occurring on quartz were made.

Figure 11 shows that the decomposition (dehydrogenation) of formic acid vapor on germanium followed zero-order kinetics in the early stages of the reaction. Above about 30 per cent decomposition, deviations from zero order occurred. However, the experimental points fitted the equation:

$$\frac{n_{CO_2}}{n_o - n_{CO_2}} = Bt \quad \text{for} \quad n_o = \text{constant} \tag{67}$$

where n_{CO_2} is the amount of carbon dioxide, n_o is the amount of monomeric formic acid present originally, B is a constant and t is the time of decomposition; Figure 16 illustrates the validity of this expression.

This equation can thus be used to help calculate consistent rate constants (e.g., at 10 per cent decomposition) from data obtained in a range of decomposition for which zero-order kinetics do not hold. For example, n_{CO_2}, n_o and t are known or calculable from experimental data. The slope (B) of the line in Equation (67) can thus be evaluated. When

$$t = \frac{0.111}{B} \tag{68}$$

the original formic acid was 10 per cent decomposed, since under these conditions, from Equation (67):

$$\frac{n_{CO_2}}{n_o - n_{CO_2}} = Bt = 0.111$$

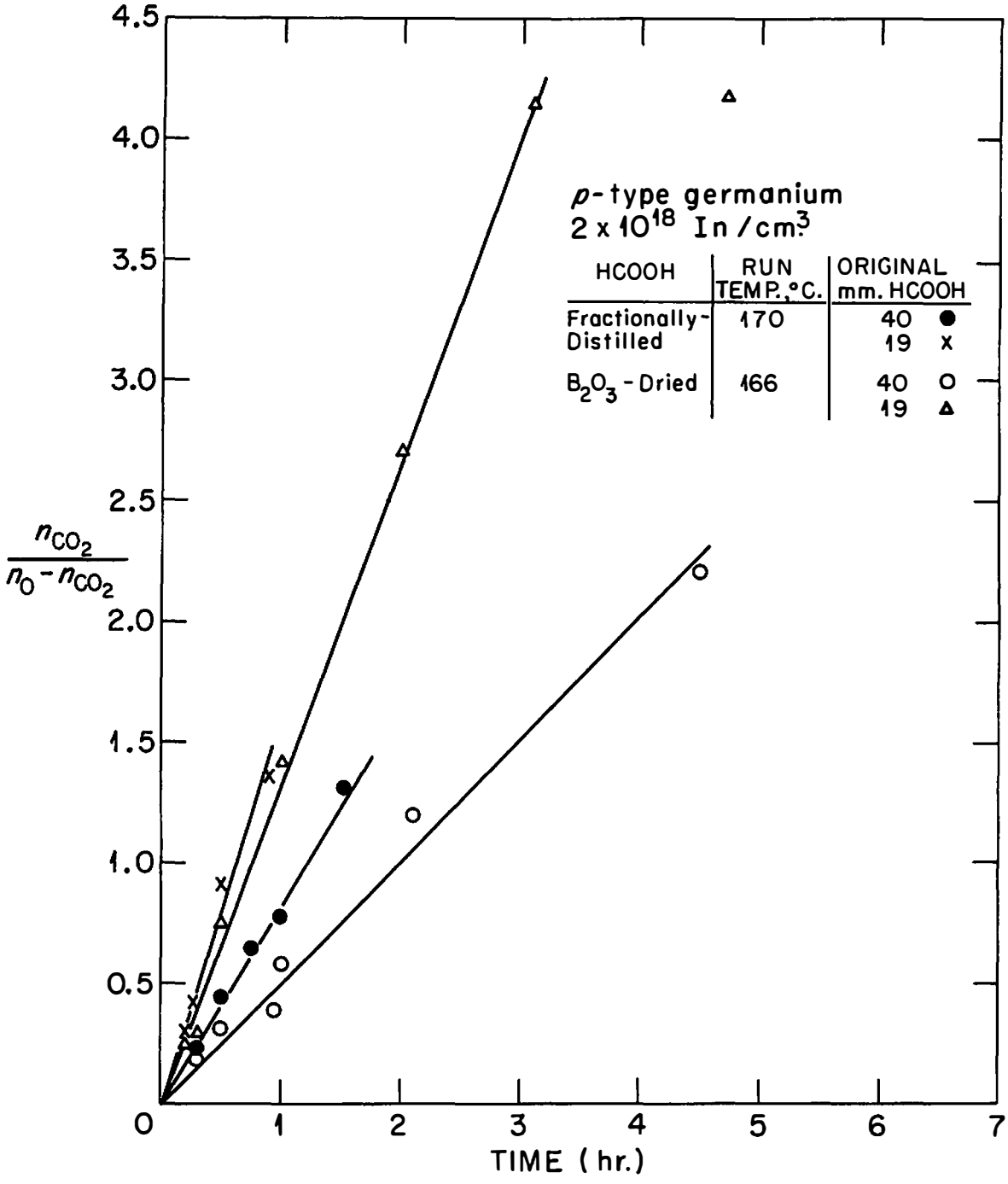

Figure 16. Empirical correlation of data on dehydrogenation of formic acid on germanium.

from which

$$\frac{n_{CO_2}}{n_o} = 0.10 = f_{CO_2} \tag{69}$$

Thus, the concentration of carbon dioxide (n_{CO_2}) and the time for 10 per cent decomposition are known from Equations (69) and (68), respectively. Figure 17 illustrates typical data uncorrected, and corrected, for the deviation from zero-order kinetic behavior.

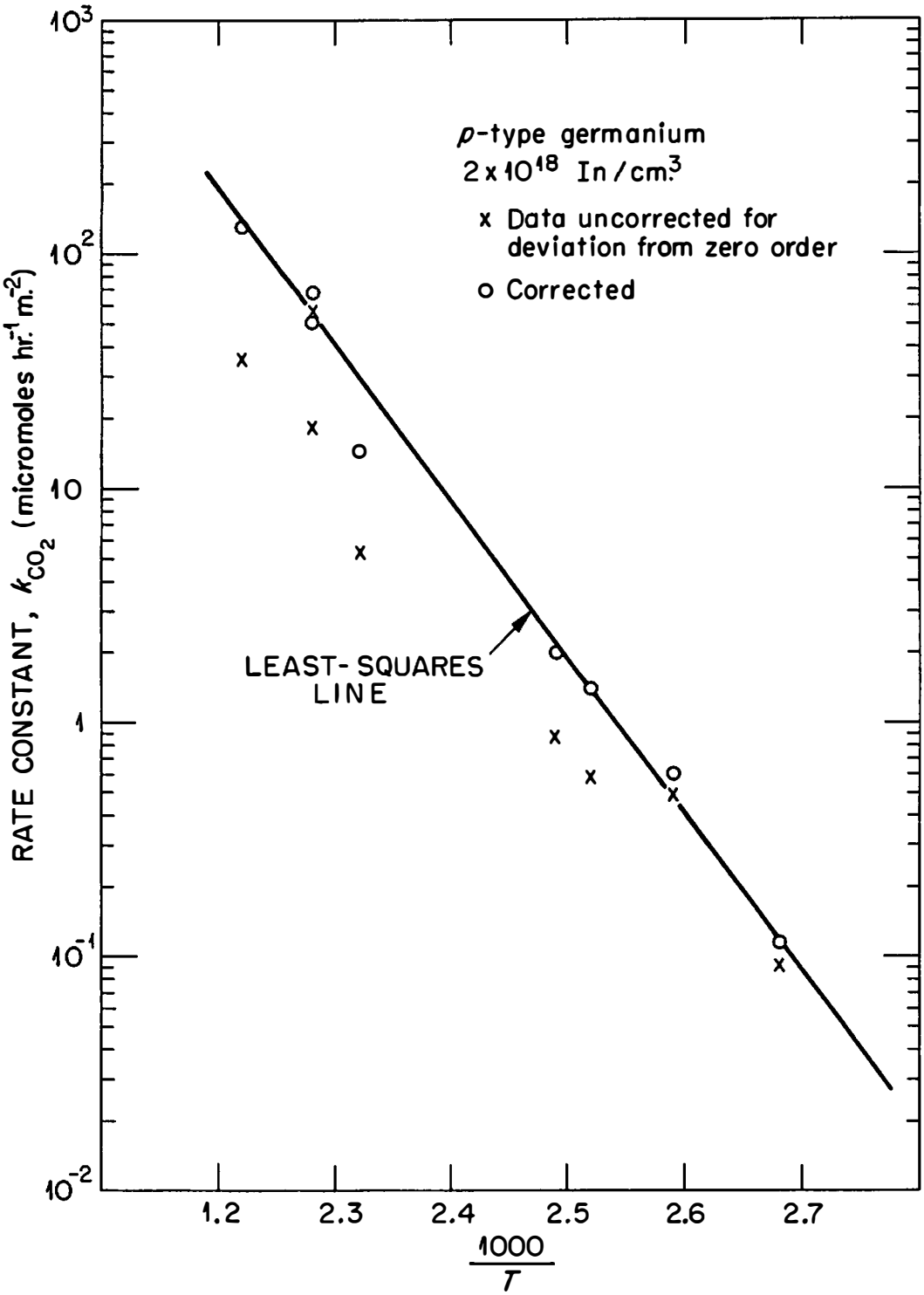

Figure 17. Typical result of correcting data on rate of dehydrogenation of formic acid for deviation from zero order.

BIBLIOGRAPHY

BIBLIOGRAPHY

1. M. Berzelius, Ann. chim. et phys., 61, 150 (1836).
2. H. S. Taylor, Advances in Catalysis, 9, 1 (1957).
3. I. Langmuir, Trans. Faraday Soc., 17, 617 (1922).
4. H. S. Taylor, Proc. Roy. Soc. (London), A108, 105 (1925).
5. H. S. Taylor, J. Am. Chem. Soc., 53, 578 (1931).
6. A. A. Balandin, Z. physik. Chem., Abt. B, 2, 289 (1929).
7. O. Beeck, A. E. Smith, and A. Wheeler, Proc. Roy. Soc. (London), A177, 62 (1940).
8. A. T. Gwathmey and R. E. Cunningham, Advances in Catalysis, 10, 57 (1958).
9. H. M. C. Sosnovsky, J. Chem. Phys., 23, 1486 (1955).
10. M. McD. Baker and G. I. Jenkins, Advances in Catalysis, 7, 1 (1955).
11. O. Beeck, Rev. Modern Phys., 17, 61 (1945).
12. M. Boudart, J. Am. Chem. Soc., 72, 1040 (1950).
13. L. Pauling, Proc. Roy. Soc. (London), A196, 343 (1949).
14. C. Herring and M. H. Nichols, Rev. Modern Phys., 21, 236 (1949).
15. G. Rienäcker, Periodica Polytech., 2, 193 (1958); C. A., 53, 13754g (1959).
16. A. K. Brewer, J. Phys. Chem., 32, 1006 (1928).
17. O. Schmidt, Chem. Revs., 12, 363 (1933).
18. J. E. Nyrop, Chem. & Ind. (London), 9, 752 (1931).
19. L. V. Pisarzhevskii, Acta Physicochim. U. R. S. S., 6, 555 (1937); C. A., 32, 4416 (1938).
20. S. Roginskii and E. Shul'tz, Z. physik. Chem., Abt. A, 138, 21 (1928).
21. J. E. Lennard-Jones, Trans. Faraday Soc., 28, 333 (1932).

22. P. H. Emmett and E. Teller, "Twelfth Report of the Committee on Catalysis," National Research Council, John Wiley and Sons, Inc., New York, N. Y., 1940, p. 68.

23. C. Wagner and K. Hauffe, Z. Elektrochem., 44, 172 (1938).

24. G. M. Schwab and G. Holz, Z. anorg. Chem., 252, 205 (1944).

25. G. M. Schwab, Discussions Faraday Soc., 8, 166 (1950).

26. D. A. Dowden, J. Chem. Soc., 242 (1950).

27. B. M. W. Trapnell, "Chemisorption," Academic Press, Inc., New York, N. Y., 1955.

28. F. S. Stone, in W. E. Garner (ed.), "Chemistry of the Solid State," Academic Press, Inc., New York, N. Y., 1955, p. 367.

29. K. Hauffe, Advances in Catalysis, 7, 213 (1955).

30. Th. Wolkenstein, Advances in Catalysis, 12, 189 (1960).

31. W. E. Garner, Bull. soc. chim. Belges, 67, 404 (1958).

32. P. J. Fensham, Quart. Revs. (London), 11, 227 (1957).

33. R. Suhrmann, Advances in Catalysis, 7, 303 (1955).

34. A. H. Wilson, Proc. Roy. Soc. (London), A133, 458 (1931); A134, 277 (1931).

35. P. B. Weisz, in R. H. Kingston (ed.), "Semiconductor Surface Physics," University of Pennsylvania Press, Philadelphia, Pa., 1957, p. 247.

36. D. G. Thomas, in N. B. Hannay (ed.), "Semiconductors," Reinhold Publishing Corp., New York, N. Y., 1959, p. 269.

37. G. M. Schwab, in R. H. Kingston (ed.), "Semiconductor Surface Physics," University of Pennsylvania Press, Philadelphia, Pa., 1957, p. 283.

38. F. S. Stone, in W. E. Garner (ed.), "Chemisorption," Academic Press, Inc., New York, N. Y., 1957, p. 181.

39. T. R. Hogness and W. C. Johnson, J. Am. Chem. Soc., 54, 3583 (1932).

40. K. Tamaru, M. Boudart, and H. Taylor, J. Phys. Chem., 59, 801 (1955).

41. P. J. Fensham, K. Tamaru, M. Boudart, and H. Taylor, J. Phys. Chem., 59, 806 (1955).

42. K. Tamaru, J. Phys. Chem., 60, 612 (1956); Bull. Fac. Eng. Yokohama Natl. Univ., 6, 81 (1957); C. A., 52, 7808e (1958).

43. H. S. Taylor, Can. J. Chem., 33, 838 (1955).

44. K. Tamaru and M. Boudart, Advances in Catalysis, 9, 699 (1957).

45. K. Tamaru, J. Phys. Chem., 61, 647 (1957).

46. G. K. Boreskov and V. L. Kuchaev, Doklady Akad. Nauk S. S. S. R., 119, 302 (1958); Problemy Kinetiki i Kataliza, 9, 61 (1957); C. A., 52, 19370a (1958).

47. Y. L. Sandler and M. Gazith, J. Phys. Chem., 63, 1095 (1959).

48. J. T. Law and E. E. Francois, Ann. N. Y. Acad. Sci., 58, 925 (1954).

49. O. V. Krylov, S. Z. Roginskii, and V. M. Frolov, Doklady Akad. Nauk S. S. S. R., 111, 623 (1956); C. A., 51, 13539c (1957); Document AEC-tr-3267 (June 6, 1958).

50. V. I. Lyashenko and I. I. Stepko, Izvest. Akad. Nauk S. S. S. R., Ser. Fiz., 21, 201 (1957); Bull. Acad. Sci. U. S. S. R., Phys. Ser., 21, 201 (1957) (English translation); C. A., 51, 11829i (1957).

51. G. P. Romanova and I. I. Stepko, Dopovidi Akad. Nauk Ukr. R. S. R., 585 (1958); C. A., 52, 16850c (1958).

52. R. M. Dell, J. Phys. Chem., 61, 1584 (1957).

53. International Hydrogenation Patents Co. Ltd., French Patent 794,437 (Feb. 17, 1936).

54. D. Maclean, et al., British Patent 795,968 (June 4, 1958).

55. G. L. Hervert and H. S. Bloch, U. S. Patent 2,820,693 (Jan. 21, 1958).

56. G. M. Schwab, G. Greger, St. Krawczynski, and J. Penzkofer, Z. physik. Chem. (Frankfurt), 15, 363 (1958).

57. V. M. Frolov, O. V. Krylov, and S. Z. Roginskii, Doklady Akad. Nauk S. S. S. R., 126, 107 (1959); C. A., 53, 21612d (1959).

58. W. H. Watson, Jr., J. Appl. Phys., 32, 120 (1961).

59. J. T. Law, J. Phys. Chem., 59, 543 (1955).

60. J. R. Ligenza, J. Phys. Chem., 64, 1017 (1960).

61. M. Green, Phys. and Chem. Solids, 14, 77 (1960).

62. M. Green, J. A. Kafalas, and P. H. Robinson, in R. H. Kingston (ed.), "Semiconductor Surface Physics," University of Pennsylvania Press, Philadelphia, Pa., 1957, p. 349.

63. A. C. Zettlemoyer, G. Srinivasan, and C. Hassis, Armed Services Technical Information Agency, Document AD-247 578 (Dec. 16, 1960); Document AD-252 048 (Mar. 9, 1961).

64. N. B. Hannay (ed.), "Semiconductors," Reinhold Publishing Corp., New York, N. Y., 1959.

65. T. H. Geballe, in N. B. Hannay (ed.), "Semiconductors," Reinhold Publishing Corp., New York, N. Y., 1959, p. 313.

66. A. K. Jonscher, "Principles of Semiconductor Device Operation," G. Bell and Sons, Ltd., London, 1960, p. 9.

67. N. B. Hannay, in N. B. Hannay (ed.), "Semiconductors," Reinhold Publishing Corp., New York, N. Y., 1959, p. 1.

68. G. Goudet and C. Meuleau, "Semiconductors; Their Theory and Practice," Macdonald and Evans Ltd., London, 1957, p. 175.

69. L. M. Dennis, K. M. Tressler, and F. E. Hance, J. Am. Chem. Soc., 45, 2033 (1923).

70. Gmelin "Handbook of Inorganic Chemistry," 8th ed., Supplement, System No. 45, Germanium, Verlag Chemie, GmbH., Weinheim/Bergstrasse, West Germany, 1958, p. 32.

71. H. L. West and G. K. Rollefson, J. Am. Chem. Soc., 58, 2140 (1936).

72. G. A. Ropp, personal communication.

73. A. A. Morton, "Laboratory Technique in Organic Chemistry," 1st ed., McGraw Hill Book Co., Inc., New York, N. Y., 1938, pp. 7-8.

74. L. H. Horsley, Anal. Chem., 19, 508 (1947).

75. H. N. Barham and L. W. Clark, J. Am. Chem. Soc., 73, 4638 (1951).

76. J. Timmermans, Physico-Chemical Constants of Pure Organic Compounds," Elsevier Publishing Co., New York, N. Y., 1950, p. 377.

77. A. S. Coolidge, J. Am. Chem. Soc., 52, 1874 (1930).

78. E. M. Levin, H. F. McMurdie, and F. P. Hall, "Phase Diagrams for Ceramists," The American Ceramic Society, Inc., Columbus, Ohio, 1956, p. 196 (Figure 561).

79. W. J. Youden, in I. M. Kolthoff and P. J. Elving (eds.), "Treatise on Analytical Chemistry," Part I, Volume I, The Interscience Encyclopedia, Inc., New York, N. Y., 1959, p. 51.

80. P. Mars, in J. H. de Boer, et al. (eds.), "The Mechanism of Heterogeneous Catalysis," Elsevier Publishing Co., New York, N. Y., 1960, p. 49.

81. W. L. Nelson and C. J. Engelder, J. Phys. Chem., 30, 470 (1926).

82. J. J. Madison, Anal. Chem., 30, 1859 (1958).

83. W. M. H. Sachtler and N. H. de Boer, J. Phys. Chem., 64, 1579 (1960).

84. J. H. Crawford, Jr., H. C. Schweinler, and D. K. Stevens, J. Appl. Phys., 27, 839 (1956).

85. K. Tamaru, Trans. Faraday Soc., 55, 824 (1959).

86. K. Tamaru, Trans. Faraday Soc., 55, 1191 (1959).

87. W. Volk, Chem. Eng., 63, 177 (1956).

88. W. M. D. Bryant, Ind. Eng. Chem., 23, 1019 (1931).

89. P. Mars, Z. physik. Chem. (Frankfurt), 22, 309 (1959).

90. J. Fahrenfort, L. L. Van Reyen, and W. M. H. Sachtler, in J. H. de Boer, et al. (eds.), "The Mechanism of Heterogeneous Catalysis," Elsevier Publishing Co., New York, N. Y., 1960, p. 23.

91. R. Suhrmann and G. Wedler, Advances in Catalysis, 9, 223 (1957).

92. C. S. Fuller, Chem. Revs., 59, 65 (1959).

93. C. S. Fuller, W. Kaiser, and C. D. Thurmond, Phys. and Chem. Solids, 17, 301 (1961).

94. J. Tuul and H. E. Farnsworth, J. Am. Chem. Soc., 83, 2253 (1961).

95. M. Boudart, J. Am. Chem. Soc., 74, 1531 (1952).

96. P. B. Weisz, J. Chem. Phys., 20, 1483 (1952).

97. P. B. Weisz, J. Chem. Phys., 21, 1531 (1953).

98. P. Aigrain and C. Dugas, Z. Elektrochem., 56, 363 (1952).

99. K. Hauffe and H. J. Engell, Z. Elektrochem., 56, 366 (1952).

100. J. A. Dillon and H. E. Farnsworth, J. Appl. Phys., 28, 174 (1957).

101. E. Wicke, Z. Elektrochem., 53, 279 (1949).

102. E. Molinari and G. Parravano, J. Am. Chem. Soc., 75, 5233 (1953).

103. A. Clark, Ind. Eng. Chem., 45, 1476 (1953).

104. G. Parravano and M. Boudart, Advances in Catalysis, 7, 47 (1955).

105. G. M. Schwab, Trans. Faraday Soc., 42, 689 (1946).

106. D. A. Dowden and P. W. Reynolds, Discussions Faraday Soc., 8, 184 (1950).

107. R. P. Eischens and W. A. Pliskin, Second International Congress on Catalysis, Paris, France, 1960, Paper 35, Section I.

108. K. Hirota, K. Kuwata, T. Otaki, and S. Asai, Second International Congress on Catalysis, Paris, France, 1960, Paper 36, Section I.

109. W. M. H. Sachtler and J. Fahrenfort, Second International Congress on Catalysis, Paris, France, 1960, Paper 37, Section I.

110. H. E. Farnsworth, D. Shooter, and J. Marsh, Armed Services Technical Information Agency, Document AD-252 769 (February 1961).

111. G. M. Schwab and E. Killmann, Z. physik. Chem. (Frankfurt), 24, 119 (1960).

112. D. A. Dowden, N. Mackenzie, and B. M. W. Trapnell, Proc. Roy. Soc. (London), A237, 245 (1956).

113. V. C. F. Holm and R. W. Blue, Ind. Eng. Chem., 44, 107 (1952).

114. L. G. Harrison and C. A. McDowell, Proc. Roy. Soc. (London), A228, 66 (1955).

115. D. D. Eley and H. Inokuchi, Z. Elektrochem., 63, 29 (1959).

116. G. M. Schwab and E. Schwab-Agallidis, J. Am. Chem. Soc., 71, 1806 (1949).

117. Z. G. Szabo, F. Solymosi, and I. Batta, Z. physik. Chem. (Frankfurt), 17, 125 (1958).

118. G. M. Schwab, J. Block, W. Müller, and D. Schultze, Naturwissenschaften, 44, 582 (1957).

119. G. M. Schwab, J. Block, and D. Schultze, Angew. Chem., 71, 101 (1959).

120. Z. G. Szabo, F. Solymosi, and I. Batta, Z. physik. Chem. (Frankfurt), 23, 56 (1960).

121. Z. G. Szabo and F. Solymosi, Second International Congress on Catalysis, Paris, France, 1960, Paper 80, Section II.

122. A. A. Frost and R. G. Pearson, "Kinetics and Mechanism," John Wiley and Sons, Inc., New York, N. Y., 1953, p. 31.

123. R. H. Fowler and E. A. Guggenheim, "Statistical Thermodynamics," The University Press, Cambridge, 1939, p. 169.

124. H. W. Woolley, R. B. Scott, and F. G. Brickwedde, J. Research Natl. Bur. Standards, 41, 379 (1948).

125. A. S. Coolidge, J. Am. Chem. Soc., 50, 2166 (1928).

126. H. C. Ramsperger and C. W. Porter, J. Am. Chem. Soc., 48, 1267 (1926).

127. W. Waring, Chem. Revs., 51, 171 (1952).

VITA

George E. Moore was born on September 28, 1922, in Evanston, Illinois. He received his primary education in Chicago and Wilmette and was graduated from high school in Winnetka, Illinois in June 1939. He attended Northwestern University in Evanston, and received a Bachelor of Science degree with honors in June 1943. He then entered the Graduate School of the University of Minnesota. In February 1944 he joined the Manhattan Project at the University of Chicago, and was transferred to Oak Ridge, Tennessee in March 1944. He has been employed by the Chemistry Division of the Oak Ridge National Laboratory since June 1944. His fields of research have been the chemistry of the heavy elements, anion exchange, nuclear reactor materials, and, recently, radiation effects and heterogeneous catalysis. He entered the Graduate School of the University of Tennessee in 1951 on a part-time basis.

The author is a member of Phi Beta Kappa, Phi Lambda Upsilon, Sigma Xi, the Research Society of America, the American Chemical Society, and the American Association for the Advancement of Science. His publications are:

"Chemistry of Plutonium (V). Potential of the Plutonium (V)/(VI) Couple. Ionic Species of Plutonium (V) in Acidic Solutions." K. A. Kraus and G. E. Moore, in G. T. Seaborg, J. J. Katz, and W. M. Manning, "The Transuranium Elements," Research Papers, National Nuclear Energy Series, Vol. 14B, Part I, McGraw-Hill Book Co., Inc., New York, N. Y., 1949, p. 550.

"Spectrophotometry of Plutonium (VI) in Perchlorate Solutions." G. E. Moore and K. A. Kraus, in G. T. Seaborg, J. J. Katz, and W. M. Manning, "The Transuranium Elements," Research Papers, National Nuclear Energy Series, Vol. 14B, Part I, McGraw-Hill Book Co., Inc., New York, N. Y., 1949, p. 608.

"Separation of Zirconium and Hafnium with Anion Exchange Resins." K. A. Kraus and G. E. Moore, J. Am. Chem. Soc., 71, 3263 (1949).

"Separation of Columbium and Tantalum with Anion Exchange Resins." K. A. Kraus and G. E. Moore, J. Am. Chem. Soc., 71, 3855 (1949).

"Adsorption of Protactinium from Hydrochloric Acid Solutions by Anion Exchange Resins." K. A. Kraus and G. E. Moore, J. Am. Chem. Soc., 72, 4293 (1950).

"Adsorption of Iron by Anion Exchange Resins from Hydrochloric Acid Solutions." G. E. Moore and K. A. Kraus, J. Am. Chem. Soc., 72, 5792 (1950).

"Anion Exchange Studies. I. Separation of Zirconium and Niobium in HCl-HF Mixtures." K. A. Kraus and G. E. Moore, J. Am. Chem. Soc., 73, 9 (1951).

"Anion Exchange Studies. II. Tantalum in Some HF-HCl Mixtures." K. A. Kraus and G. E. Moore, J. Am. Chem. Soc., 73, 13 (1951).

"Anion Exchange Studies. III. Protactinium in Some HCl-HF Mixtures: Separation of Niobium, Tantalum and Protactinium." K. A. Kraus and G. E. Moore, J. Am. Chem. Soc., 73, 2900 (1951).

"Anion Exchange Studies. IV. Cobalt and Nickel in Hydrochloric Acid Solutions." G. E. Moore and K. A. Kraus, J. Am. Chem. Soc., 74, 843 (1952).

"Anion Exchange Studies. V. Adsorption of Hydrochloric Acid by a Strong Base Anion Exchanger." K. A. Kraus and G. E. Moore, J. Am. Chem. Soc., 75, 1457 (1953).

"Anion Exchange Studies. VI. The Divalent Transition Elements Manganese to Zinc in Hydrochloric Acid." K. A. Kraus and G. E. Moore, J. Am. Chem. Soc., 75, 1460 (1953).

"Anion Exchange Studies. XV. Separation of Protactinium and Iron by Anion Exchange in HCl-HF Solutions." K. A. Kraus and G. E. Moore, J. Am. Chem. Soc., 77, 1383 (1955).

"Anion Exchange Studies. XVII. Molybdenum(VI), Tungsten(VI) and Uranium(VI) in HCl and HCl-HF Solutions." K. A. Kraus, F. Nelson, and G. E. Moore, J. Am. Chem. Soc., 77, 3972 (1955).

"Anion Exchange Studies. XXI. Th(IV) and U(IV) in Hydrochloric Acid. Separation of Thorium, Protactinium and Uranium," K. A. Kraus, G. E. Moore, and F. Nelson, J. Am. Chem. Soc., 78, 2692 (1956).

"The Use of Ionizing Radiation in Heterogeneous Catalysis." E. H. Taylor, H. W. Kohn, and G. E. Moore, in "Large Radiation Sources in Industry," Volume II, International Atomic Energy Agency, Kärntner Ring, Vienna 1, Austria, 1960, p. 119.